NRC Research and/or Technical Assistance Rept

P0E

EGG-NTAP-6030
September 1982

BEST ESTIMATE ANALYSIS OF A LARGE BREAK LOCA IN A RESAR-3S PRESSURIZED WATER REACTOR

C. A. Dobbe

Idaho National Engineering Laboratory
Operated by the U.S. Department of Energy

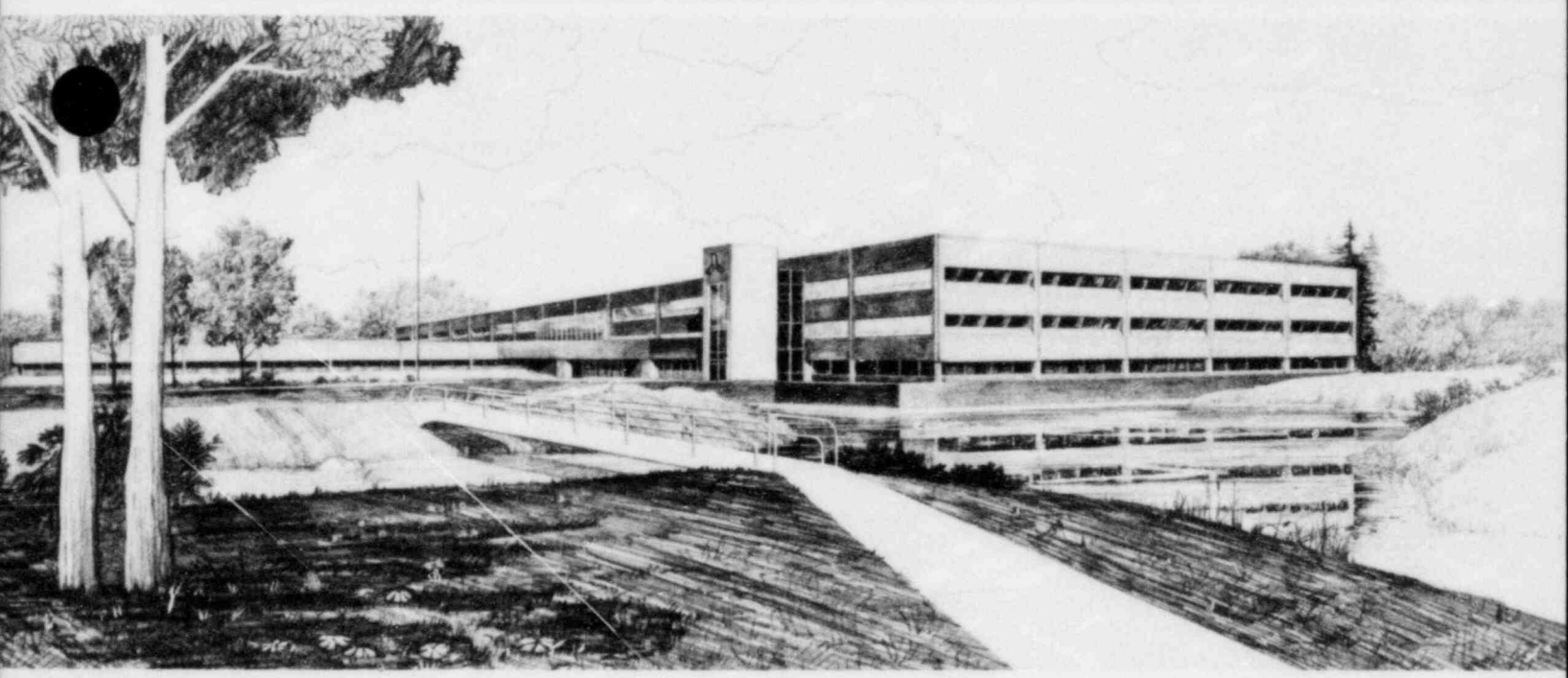

This is an informal report intended for use as a preliminary or working document

Prepared for the
U.S. NUCLEAR REGULATORY COMMISSION
Under DOE Contract No. DE-AC07-76ID01570
FIN No. A6468

EG&G Idaho

EG&G Idaho, Inc.

FORM EG&G-398
(Rev. 03-82)

INTERIM REPORT

Accession No. _____

Report No. EGG-NTAP-6030

Contract Program or Project Title: NRC Technical Assistance Program Division

Subject of this Document: Best Estimate Analysis of a Large Break LOCA in a RESAR-3S Pressurized Water Reactor

Type of Document: Technical Report

Author(s): C. A. Dobbe

Date of Document: September 1982

Responsible NRC Individual and NRC Office or Division: J. Guttmann, NRC-DSI

This document was prepared primarily for preliminary or internal use. It has not received full review and approval. Since there may be substantive changes, this document should not be considered final.

EG&G Idaho, Inc.
Idaho Falls, Idaho **83415**

Prepared for the
U.S. Nuclear Regulatory Commission
Washington, D.C.
Under DOE Contract No. **DE-AC07-76ID01570**
NRC FIN No. A6468

INTERIM REPORT

ABSTRACT

An analysis was performed to determine the consequences resulting from a large cold leg break loss-of-coolant accident in a Westinghouse RESAR-3S nuclear steam supply system. The TRAC-PD2 computer code was used to calculate the effects of the large cold leg break assuming best estimate plant initial and boundary conditions. Results of the calculation were compared to the limiting large break Westinghouse licensing analysis to verify and quantify the conservatisms inherent in licensing analyses. The comparisons show a high degree of conservatism present in licensing assumptions and analytical techniques.

FIN No. A6468--RESAR-3S "Most Probable" Best Estimate
LOCA Analyses in Support of FSAR Reviews

SUMMARY

An analysis was performed to determine the consequences resulting from a large break loss-of-coolant accident in a Westinghouse RESAR-3S nuclear steam supply system. The analysis was performed with the TRAC-PD2 computer code assuming best estimate initial and boundary conditions. Results of the analysis were compared to the Westinghouse licensing analysis of the limiting large break to verify and quantify the conservatisms inherent in licensing analyses.

The large break analysis performed with the TRAC-PD2 computer code considered a 200% double-ended offset shear of a cold leg pipe. The calculation was terminated after 50.8 s of the transient. The reactor vessel voided during blowdown and was refilled by 45 s. Core wide cladding surface temperature heatup was calculated to occur during the initial 2.5 s of the transient with a predicted core wide rewet away from the high power regions of the core predicted between 2.5 and 5 s. The calculated peak cladding temperature of 1085°F was calculated to occur 2.5 s after the break and complete quenching of the core was calculated to occur 46 s after break.

Comparisons to the Westinghouse licensing analysis showed a high degree of conservatism in the assumptions used for licensing analysis. Lower core flow, higher peak power, and higher stored energy in the Westinghouse analysis resulted in calculated peak cladding temperatures 987°F higher than predicted by the TRAC-PD2 analysis. The peak temperature in the Westinghouse calculation occurred at 155 s after the break which was during the reflood phase of the transient.

FOREWORD

This project, RESAR-3S "Most Probable" Best Estimate LOCA Analyses in Support of FSAR Reviews, was conducted under the direction of NRC's Division of Systems Integration, Roger Mattson, Director; Themis Speis, Assistant Director for Reactor Safety; Brian Sheron, Branch Chief for Reactor Systems; Norm Lauben, RSB Section Leader; and Jack Guttmann, Project Manager/Technical Monitor. EG&G personnel involved in the project were Tom Charlton, Branch Manager, Reactor Simulation and Analysis Branch; Andy Peterson, Supervisor, PWR Systems Analysis; Tom Laats, Supervisor, Fuels Analysis and Data Bank; Charles Dobbe and Jay Larson, Engineers; Joan Mosher, Glada Gatenby, Kim Culbertson, Brenda Hendrickson, and Dorothy Cullen, Word Processing. Completed in September of 1982, this project was performed under FIN Number A6468 and NRC B&R Number 20 19 40 42 3.

ACKNOWLEDGMENTS

The author gratefully acknowledges the assistance of Jay Larsen in developing the TRAC-PD2 input deck used for the analysis. The assistance of Thad Knight and the Safety Code Development staff at Los Alamos National Laboratory was invaluable in the performance of the calculation. The critical review and advice of Andy Peterson plus the efficient work and patience of Joan Mosher, Glada Gatenby, Kim Culbertson, Brenda Hendrickson, and Dorothy Cullen were greatly appreciated during preparation of this report.

CONTENTS

ABSTRACT ii

SUMMARY iii

FOREWORD iv

ACKNOWLEDGMENTS v

1. INTRODUCTION 1

2. COMPUTER CODE DESCRIPTION 3

3. SPECIFICATION OF ANALYSIS 4

3.1 RESAR-3S System Description 4

3.2 Transient Sequence of Events 7

4. TRAC-PD2 INPUT MODEL 9

4.1 Nodalization Scheme 9

4.2 Code Options 15

5. ANALYTICAL RESULTS 17

5.1 TRAC-PD2 Steady State Analysis 17

5.2 TRAC-PD2 Transient Analysis 22

5.3 Comparison to Licensing Analysis 35

6. CONCLUSIONS 45

REFERENCES 46

APPENDIX A--TRAC-PD2 UPDATES USED FOR THE RESAR-3S CALCULATION A-1

APPENDIX B--FRAPCON-2 ANALYSIS FOR INITIAL FUEL CONDITIONS B-1

APPENDIX C--QUALITY ASSURANCE PROCEDURE FOR DEVELOPMENT OF THE TRAC-PD2 RESAR-3S LARGE BREAK MODEL C-1

FIGURES

1. TRAC-PD2 model of the RESAR-3S coolant loops 10

2. TRAC-PD2 model of the RESAR-3S reactor vessel 12

3. Steady state calculation of hot leg fluid temperature 18

4. Steady state calculation of cold leg fluid temperature 18

5. Steady state calculation of core inlet mass flow rate 19

6. Steady state calculation of pressurizer surge line flow 19

7. Steady state calculation of average core pressure 20

8. Steady state calculation of steam generator steam dome pressure 20

9. Comparison of calculated and desired fuel pin hot spot radial temperature profiles 21

10. Calculated pressure response in the pressurizer and upper plenum 26

11. Calculated pump side break flow 28

12. Calculated vessel side break flow 28

13. Calculated mass flow rate in the loop 1 cold leg 29

14. Calculated core inlet mass flow rate 31

15. Calculated liquid fraction in the lower plenum and core 32

16. Calculated hot pin cladding surface temperature response 32

17. Calculated high power region cladding surface temperature response 33

18. Calculated low power region cladding surface temperature response 33

19. Comparison of upper plenum pressure predictions for the TRAC-PD2 and the Westinghouse analyses 36

20. Comparison of pump side break mass flow predictions for the TRAC-PD2 and the Westinghouse analyses 36

21. Comparison of vessel side break mass flow predictions for the TRAC-PD2 and the Westinghouse analyses 37

22. Comparison of total intact loop accumulator flow predictions for the TRAC-PD2 and the Westinghouse analyses 39

23. Comparison of total intact loop ECC flow (pumped and accumulator) predictions during reflood for the TRAC-PD2 and the Westinghouse analyses 39

24. Comparison of core inlet mass flow predictions for the TRAC-PD2 and the Westinghouse analyses 41

25. Comparison of core reflooding rate predictions during reflood for the TRAC-PD2 and the Westinghouse analyses 42

26. Comparison of core liquid level predictions during reflood for the TRAC-PD2 and the Westinghouse analyses 42

27. Comparison of cladding surface temperature predictions at the 6.0 foot elevation for the TRAC-PD2 and the Westinghouse analyses 43

28. Comparison of cladding surface temperature predictions at the 7.5 foot elevation for the TRAC-PD2 and the Westinghouse analyses 43

TABLES

1. Initial plant operating conditions for the RESAR-3S NSSS 5

2. Initial axial power distribution for the RESAR-3S NSSS 5

3. Comparison of calculated and desired initial conditions for the RESAR-3S DECLG LOCA 23

4. Sequence of events for RESAR-3S DECLG LOCA 25

BEST ESTIMATE ANALYSIS OF A LARGE BREAK LOCA IN A RESAR-3S PRESSURIZED WATER REACTOR

1. INTRODUCTION

Present requirements for determining the acceptability of emergency core cooling (ECC) systems in light water reactors during postulated loss-of-coolant accidents (LOCA) incorporate conservatisms developed to bound the uncertainties in the analytical methodology used. These conservatisms are codified in 10 CFR 50.46 and Appendix K to 10 CFR Part 50 and require conservative analytical methodology and "worst case" operating conditions, protective system failures, and break geometry. The following report documents one part of an overall effort by the Nuclear Regulatory Commission (NRC) to verify and quantify the conservatisms inherent in the requirements of 10 CFR 50.

This report documents the results of a postulated double-ended cold leg guillotine break (DECLG) LOCA analysis in a Westinghouse pressurized water reactor (PWR) assuming most probable operating parameters and utilizing state-of-the-art analytical methodology. The PWR design selected was the Westinghouse RESAR-3S nuclear steam supply system (NSSS). Westinghouse supplied as-built drawings and plant data were used to construct computer models representing the "best-estimate" of actual system geometry and operating conditions. The computer code selected for the analysis was the TRAC-PD2 computer code[2] developed at Los Alamos National Laboratory. Section 2 of this report contains a detailed description of the TRAC-PD2 computer code and justification for its use as an advanced best-estimate analytical tool.

A description of the RESAR-3S NSSS and the DECLG LOCA assumed are presented in Section 3. Details of the TRAC-PD2 nodalization used to represent the RESAR-3S system are given in Section 4 along with the user defineable options of the TRAC-PD2 computer code selected for the analysis. The results of both steady state and transient analysis are presented in Section 5. Qualitative and quantitative comparisons to the limiting licensing analysis performed by Westinghouse under the guidelines

of 10 CFR 50 are also presented in Section 5. Section 6 details the conclusions reached concerning the TRAC-PD2 analysis and the comparisons made to the Westinghouse licensing analysis.

2. COMPUTER CODE DESCRIPTION

The basic computer code used for the RESAR-3S DECLG break LOCA analysis was TRAC-PD2/MOD1,[2] identified as Version 27.0, with updates. Version 27.0 corresponds to the most recent released version and is currently being used for independent assessment at Los Alamos National Laboratory (LANL). TRAC is an advanced best-estimate computer code developed at LANL for the analysis of postulated accidents in light water reactors. The TRAC-PD2 version provides analytical capability for PWRs and scaled thermal-hydraulic experimental facilities. The code features a three dimensional treatment of the pressure vessel with one-dimensional two fluid treatment of the associated piping. The code also features a reflood tracking capability for bottom reflood and falling film quench front. The code also has the capability to generate a consistant set of initial conditions. A complete description of the thermal-hydraulic models and numerical solution methods used in the code along with detailed programming and user information are given in Reference 2. A listing and description of the updates used for the subject analysis are presented in Appendix A.

The TRAC-PD2 computer code was determined to be the most appropriate computer program for the best-estimate analysis of the consequences resulting from a DECLG LOCA. The codes ability to provide a consistant treatment of the entire accident sequence utilizing two-phase nonequilibrium numerics made it the only advanced code with demonstrated capability of evaluating a large break transient through blowdown and reflood. Independent assessment results indicates that the TRAC-PD2 computer code can predict peak clad temperatures in a large break LOCA within accuracy limits of ±144°F (two standard deviations).[3] The assessment work involved comparisons with fifteen different integral systems tests simulating blowdown, reflood and full LOCA scenarios. Finally, the multi-dimensional calculational capability in the pressure vessel allowed detailed analysis of emergency core cooling bypass and penetration as well as asymmetric core thermal-hydraulic phenomena.

3. SPECIFICATION OF ANALYSIS

The following sections of the report present details of the RESAR-3S plant as modeled and the DECLG LOCA scenario assumed. Where appropriate, comparisons to the Westinghouse licensing analysis of the DECLG LOCA are presented.

3.1 RESAR-3S System Description

The RESAR-3S NSSS is a Westinghouse pressurized water reactor design consisting of a pressure vessel containing the nuclear fuel and four closed reactor coolant loops connected in parallel to the pressure vessel. Each loop contains a reactor coolant pump, steam generator, and emergency core cooling systems (ECCS) with one loop connected to an electrically heated pressurizer. The reactor coolant pumps are Westinghouse vertical, single-stage, centrifugal pumps of the shaft-seal type. The steam generators are Westinghouse vertical U-tube units containing inconel tubes.

The nuclear core consists of 193 fuel assemblies each containing 264 fuel pins in a 17 x 17 matrix. The core uses multi-region loading with an initial loading pattern utilizing three fuel enrichments arranged to achieve an optimum power distribution. Reactor control is accomplished with absorber rod cluster assemblies connected to top mounted drive assemblies moving within guide tubes in selected fuel assemblies.

Table 1 summarizes the initial operating conditions assumed for the RESAR-3S plant. The best-estimate values were used for the TRAC-PD2 analysis. These values were taken from Westinghouse plant library data and represent best estimate steady state plant parameters. The values listed for the Westinghouse licensing calculation were derived from analytical results in the form of graphical data. This data was transmitted to INEL from Westinghouse and represents the most recent Westinghouse limiting large break licensing analysis. The axial power distribution used for the TRAC-PD2 analysis is presented in Table 2. The Westinghouse licensing analysis assumed a chopped cosine distribution with an axial peaking factor of 1.45.

TABLE 1. INITIAL PLANT OPERATING CONDITIONS FOR THE RESAR-3S NSSS

Parameter	Best Estimate	Licensing
Core power	3411.	3479.[a]
Peak linear power (kW/ft)	9.13	12.62[a]
Total peaking factor	1.678	2.32[a]
Axial peaking factor	1.19	1.45[a]
Accumulator water volume (ft^3/accumulator)	1046.1	950.[a]
Accumulator gas pressure (psia)	600.0	600.0
Initial loop flow (lb/s)	38,938.	39,034.
Cold leg temperature (°F)	557.6	556.0
Core outlet temperature (°F)	621.1	not available
Hot leg temperature (°F)	617.8	617.5
Reactor coolant pressure (psia)	2250.	2280.
S.G. steam pressure (psia)	990.	982.

a. Values shown were taken from Section 15.4 of the RESAR-3S Safety Evaluation Report for comparative purposes and are believed to be representative of the values used for the current Westinghouse licensing analysis.

TABLE 2. INITIAL AXIAL POWER DISTRIBUTION FOR THE RESAR-3S NSSS

Elevation (ft above bottom of active fuel)	Normalized Power
0.00	0.27
1.20	0.97
2.40	1.13
3.60	1.19
4.80	1.19
6.00	1.19
7.20	1.18
8.40	1.14
9.60	1.10
10.80	0.91
12.00	0.22

3.2 Transient Sequence of Events

The sequence of events following a postulated DECLG LOCA are presented in this section. Differences between the Westinghouse licensing analysis and the subject TRAC-PD2 analysis are identified where applicable.

The system was assumed to be in an equilibrium condition at the beginning of the LOCA. As discussed in Section 3.1, the two analyses differ in assumed initial operating conditions. At the inception of the break, the Westinghouse licensing analysis assumed loss of offsite power and, consequently, trip of the reactor coolant pumps. The TRAC-PD2 analysis assumed offsite power was available and the primary coolant pump motors remained energized. Within the first few seconds of the blowdown, the reactor trip signal was generated on high pressurizer pressure and the safety injection (SI) signal was generated on high containment pressure. The TRAC-PD2 analysis assumed an additional 1.5 s SI signal processing time delay prior to enabling pumped safety injection. The loss of offsite power in the Westinghouse licensing analysis delayed safety injection pump startup by the 20 to 30 s required to establish onsite diesel generator power.

The SI signal also actuated a feedwater isolation signal which isolated normal feedwater flow by closing the main feedwater isolation valves. The high containment pressure condition that generated the SI signal also signaled main steamline isolation via closure of the main steam line isolation valves. The TRAC-PD2 analysis assumed the feedwater and steamline isolation signals were received simultaneously and that both valves close linearly on 5.0 s ramps. The Westinghouse licensing assumptions concerning feedwater and steamline isolation indicated secondary side isolation within 5 s after the break in the Westinghouse licensing analysis. The feedwater isolation signal initiates emergency feedwater flow by starting the auxiliary feedwater pumps. The TRAC analysis assumed auxiliary feedwater flow was available 28 s after SI signal initiation. The Westinghouse licensing analysis also assumes auxiliary feedwater flow availability.

When the primary coolant system depressurized below 600 psia accumulator injection began in both analysis. The TRAC-PD2 analysis set the accumulator water level at its nominal level whereas the Westinghouse licensing analysis selected the minimum operating level (see Table 1). After the accumulators empty, long term cooling was supplied by ECCS pumps utilizing the refueling water storage tanks (RWST) and containment sumps for water supply. Supply water temperature used in the TRAC-PD2 analysis was initially set at 60°F, the average value of RWST temperature. The temperature was changed during the transient for reasons discussed in Section 5.2. ECCS temperature for the Westinghouse licensing analysis was 90°F for the accumulator and 50°F for the refueling water storage tank, used as the source for pumped ECCS.

During the postulated LOCA, the core power was derived from decay heat. The TRAC-PD2 analysis assumed decay heat based on 90% of the ANS 73 model (see Appendix B). The Westinghouse licensing analysis assumed decay heat based on 120% of the ANS 73 model.

4. TRAC-PD2 INPUT MODEL

The TRAC-PD2 nodalization scheme developed and the user-selected code options used for the RESAR-3S DECLG LOCA analysis are described in this section. The model was developed under the guidelines given in Appendix C.

4.1 Nodalization Scheme

The steady state nodalization for the RESAR-3S plant deck consisted of four separate coolant loops and a vessel. The coolant loops were represented by 66 one-dimensional components containing 261 computational cells as illustrated by Figure 1. The four coolant loops are identical with additional components representing the pressurizer and surge line attached to the loop designated as the pressurizer loop (note also the replacement of the hot leg PIPE component in the pressurizer loop with a TEE component to provide a connection for the pressurizer). One of the non-pressurizer loops was arbitrarily selected to be the broken loop.

Each steam generator was a Westinghouse F-type design and was modeled with six components representing a feedwater source, downcomer, boiler region, steam separator, steam line, and pressure boundary. The boiler region was modeled with a STGEN component representing the tube bundle (primary and secondary side) and primary inlet and outlet plena. The downcomer region and the steam separator regions were both modeled by TEE components with the side tubes connected to allow for recirculation flow. The steamline was modeled with a VALVE component connected to a BREAK component for secondary side pressure control. A FILL component provides feedwater flow to the secondary side downcomer.

The primary coolant pumps were Westinghouse Model 93A and were each modeled with a two cell PUMP component. Westinghouse supplied data were used for single phase and fully degraded two phase input for the normal pump and normal turbine portions of the homologous head and torque curves. Semiscale pump data[4] were used to extend the fully degraded data into the

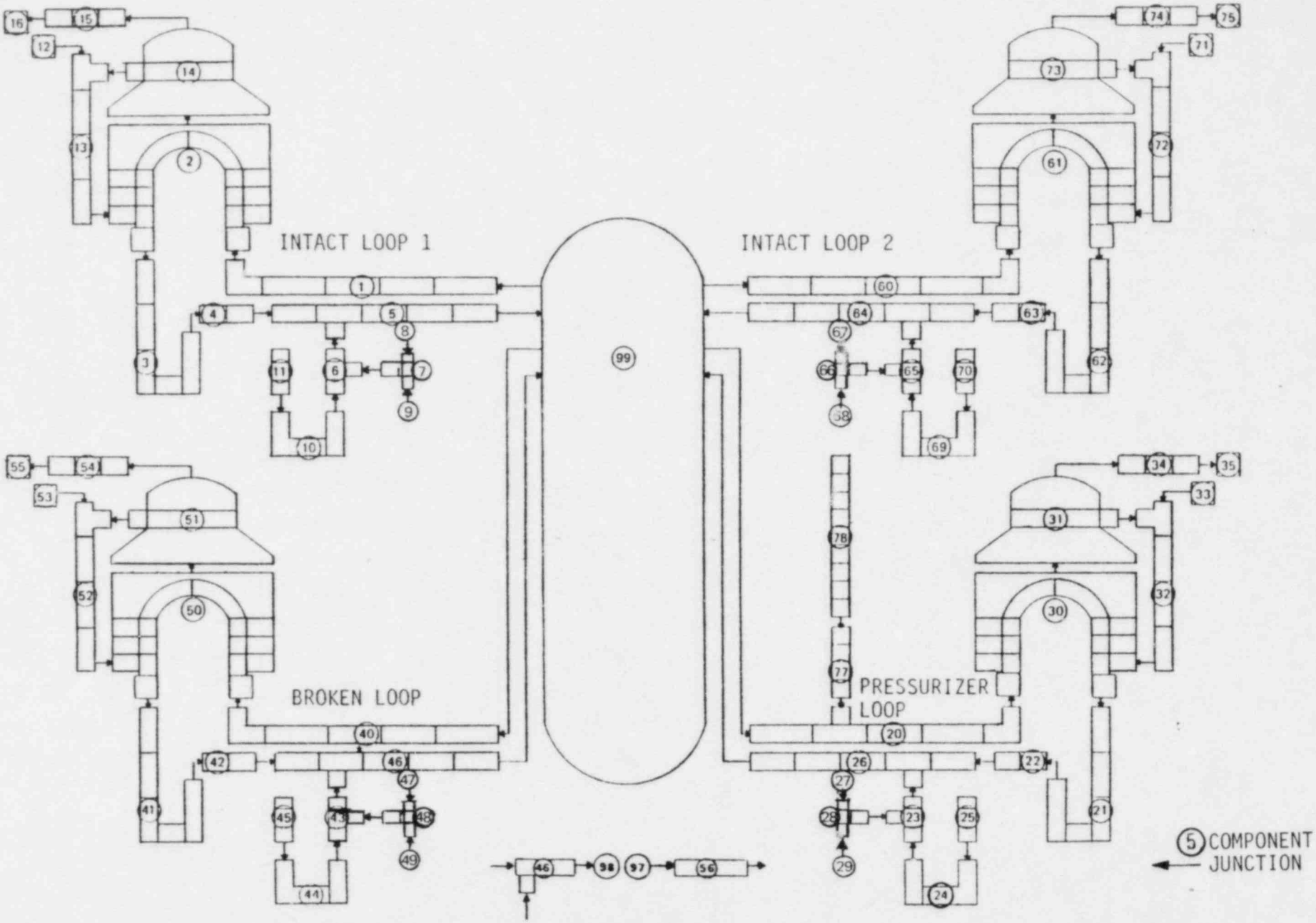

Figure 1. TRAC-PD2 model of the RESAR-3S coolant loops.

energy dissipation quadrant of the homologous curves. The RESAR-3S pumps are designed with reverse locks precluding the need for reverse pump quadrant data.

The emergency core cooling system (ECCS) simulation for each loop consists of an accumulator (ACCUM component), accumulator injection line (VALVE component and TEE component between accumulator and cold leg) and pumped ECCS systems (two FILL components connected to a TEE component connected via side legs to the accumulator injection line TEE component). The pumped ECCS systems included charging and residual heat removal systems modeled as one mass flow as a function of pressure FILL component and the safety injection system modeled as the second mass flow as a function of pressure FILL component. Charging and residual heat removal systems were combined since the actuation and delay times were the same for those two systems for the postulated DECLG LOCA analysis. The mass flow as a function of pressure data used represented best estimate pump flow data with a flow division between the intact loops and the broken loop based on the broken loop ECC line spilling to 40 psia containment backpressure. The flow split between the intact loops and broken loop reflects the fact that the ECCS ports are tied together by common headers making the flow dependent not only on the injection point pressure but also on the pressure differential between loops.

Wall heat transfer from the primary coolant pipe wall to the fluid was calculated for all primary piping except the ECCS systems. Three conduction nodes were used in the pipe wall with the outer surface assumed insulated.

The pressure vessel nodalization is shown schematically in Figure 2. The nodalization utilized a VESSEL component containing 15 axial levels, three radial rings, and four azimuthal segments yielding 180 three-dimensional computational cells and 12 nested PIPE components containing 40 one-dimensional computational cells. The boundary between the inner two radial rings bisect the radial dimension between the vessel centerline and the outer surface of the core barrel. Two rings were selected for accurate representation of the core region radial power

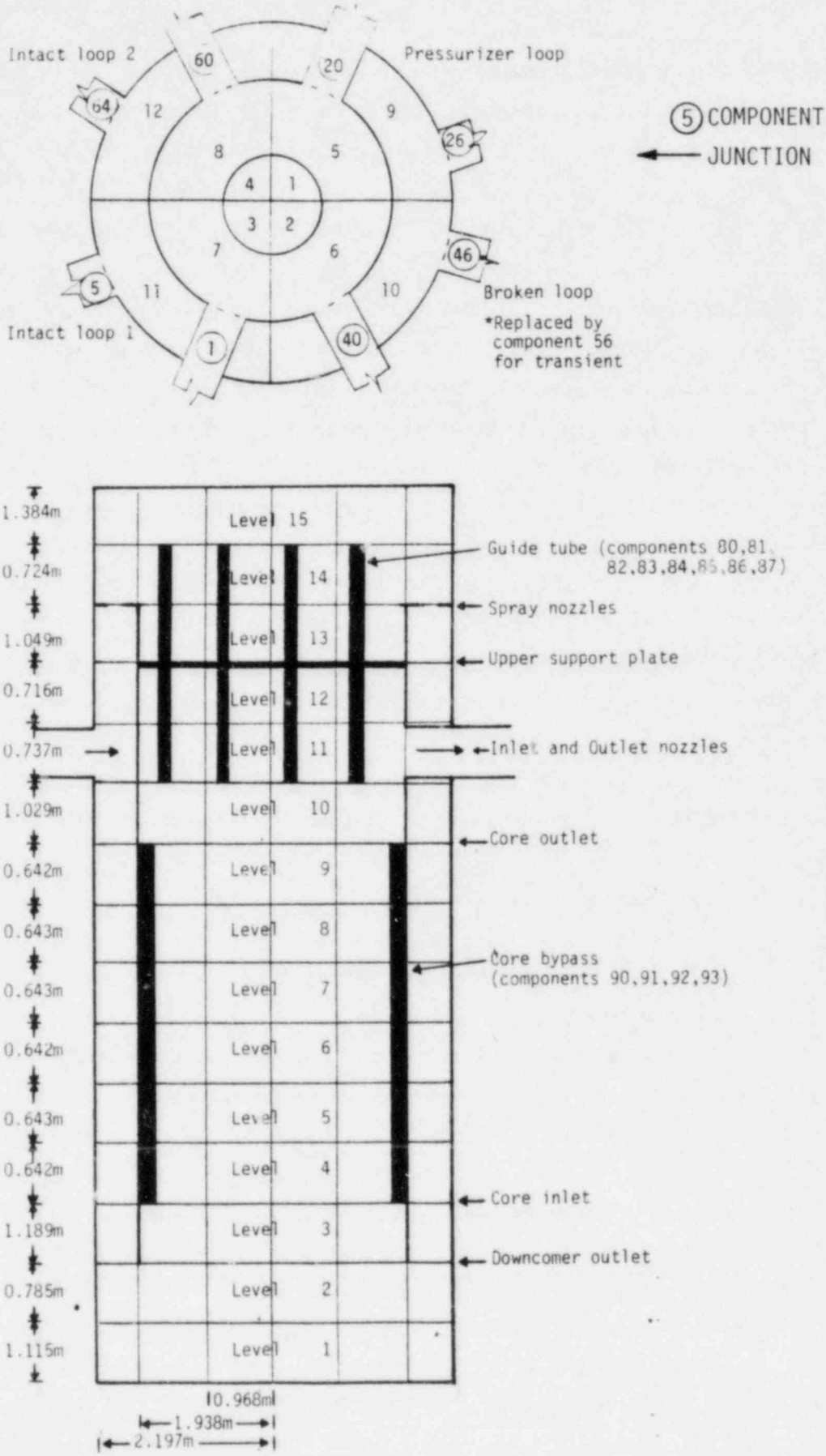

Figure 2. TRAC-PD2 model of the RESAR-3S reactor vessel.

definition. The outer ring included the volume between the outer surface of the core barrel and the inner surface of the pressure vessel at its widest dimension. The azimuthal segments each represent a 90° section of the vessel. Four azimuthal segments were required to allow source connections to the four primary coolant loops.

The axial segmentation was selected to delineate dissimilar geometric regions within the pressure vessel and to provide accurate representation of regions where thermal stratification or non-uniform fluid behavior are anticipated. The lower plenum region was represented by Levels 1 through 3. The top of Level 1 corresponded to the intersection of a vertical projection from the outside of the core barrel and the pressure vessel. The top of Level 2 was placed at the bottom of the downcomer. Level 3 terminated at the bottom of the fuel pins and constituted the core inlet.

The core height was defined as the length of the fuel pins and included Level 4 through Level 9. The levels split the core into six equal axial volumes. The volume between the core barrel and the baffle plates (referred to as the "core bypass") was represented by four PIPE components connecting Level 3 to Level 10 at each azimuthal segment of the outer core ring. The four core bypass components represented the flow path for all identified core bypass flow except spray nozzle flow for upper head cooling which was explicity modeled. Core bypass includes control rod guide thimble flow, leakage around the hot leg nozzles, flow through the barrel-baffle region, and flow in the gaps between peripherial fuel elements and the adjacent baffle wall.

The upper plenum was modeled with three levels. Level 10 included the volume between the top of the fuel pins and the bottom of the hot leg nozzle. The height of Level 11 was set equal to the inside diameter at the hot leg nozzle. Level 12 included the volume between the top of the hot leg nozzle and the horizontal centerline of the upper support plate. The upper support plate is a flow barrier between the upper plenum and the upper head and is penetrated only by the control rod guide tubes.

The upper head was modeled with three levels. Level 13 included the region above the upper support plate centerline and below the downcomer ledge. The volume between the downcomer ledge and the top of the guide tubes was modeled with Level 14. The remainder of the upper head was represented by Level 15.

The flow between the upper head and the upper plenum was modeled with the guide tube pipe components. One pipe component was modeled for each of the eight segments in the inner two rings. Each pipe component geometrically modeled all of the guide tubes that physically exist in that segment. The guide tubes connect the upper head at the bottom of Level 15 to the upper plenum at the top of Level 10.

The spray nozzle flow is physically accomplished through 32 spray nozzles penetrating the downcomer ledge. The nozzles were modeled by inputting an upper face flow area equivalent to eight nozzles at the top of Level 13 in Ring 3 in each of the four azimuthal sections.

Heat transfer in the pressure vessel included both sensible heat from internal metal mass and heat generation from nuclear fuel. The sensible heat was modeled with the lumped parameter heat slab option available for VESSEL components. A 2 cm effective thickness was used for calculating volumes of the various structures for heat transfer purposes. This effective thickness is recommended by LANL for transients of approximately 60 s. Since TRAC-PD2 only allows one material to be specified for the lumped parameter model, all internals were assumed to be 304 stainless steel, the predominanent material in the pressure vessel.

The nuclear fuel model developed was based on Westinghouse 17 x 17 standard fuel assemblies assuming cold clean dimensions (see Appendix B). The fuel pins were represented by seven conduction nodes in the fuel, one node in the gap, and two nodes in the cladding. The total number of fuel pins in each section of the core was modeled with a single fuel rod yielding eight rods transfering heat into the vessel. The innermost ring, modeling the hot channel of the core, contained an

additional computational "hot pin" in each azimuthal segment which represented the highest power pin (radially) in the core. These computational fuel rods do not feed back directly to the fluid-dynamics analysis but, instead, utilize the local fluid conditions to obtain rod temperature histories. The radial power profile was set to the values specified in Appendix B.

The broken loop cold leg nodalization was modified at the initiation of the transient to represent a double-ended offset shear break. The break was assumed to occur at the biological shield downstream of the ECCS injection port 9 ft from the cold leg nozzle. The broken loop cold leg was split into TEE component 46, containing 16 computational cells representing the pump side of the break, and PIPE component 56, containing 15 computional cells representing the vessel side of the break. Two BREAK components, 97 and 98, were added to represent containment back pressure on the vessel side and pump side of the break, respectively. The nodalization is shown schematically at the bottom of Figure 1.

4.2 Code Options

The following user defineable options of the TRAC-PD2 computer code were used for the RESAR-3S DECLG LOCA analysis. These options are recommended for use in Reference 2.

1. Wall friction was calculated with the homogeneous friction factor option (NFF=1). Abrupt area changes at the reactor vessel nozzles, pump inlet and outlet, steam generator inlet and outlet plenna, steam generator tube sheet inlet and outlet, steam separator internal junctions, and accumulator outlet utilized the automatic calculation of form-loss based on sharp-edge area change in addition to the homogeneous friction factor model calculated wall friction (NFF=-1)

2. The semi-implicit flow equations (IHYDRO=0) were used in all one-dimensional components for the steady state calculations. The fully implicit finite difference equations (IHYDRO=1) were specified for the broken loop cold leg components as nodalized for the transient calculation to accomodate the high velocities encountered near the break during blowdown.

3. The air-water option was set to treat all gas in the system as water vapor (IEOS=0).

4. Homogeneous nucleation minimum stable film boiling temperature was selected (ITMIN=0).

5. The TRAC-PD2 water packing option was used for the transient calculation (IPAK=1).

6. The CHF calculation was performed for all components (ICHF=1).

5. ANALYTICAL RESULTS

The following sections document the results of the TRAC-PD2 steady state and transient calculations and provide comparisons between the TRAC-PD2 and Westinghouse licensing calculational results.

5.1 TRAC-PD2 Steady State Analysis

A steady state calculation was run using the nodalization presented in Section 4.1 and the generalized steady state option in TRAC-PD2. The code version used was Version 27.0 with the updates identified in Appendix A as TKVALVE and GEO. The calculation was run for 83.2 s requiring 0.65 cpu hours on a CDC 7600.

The hot and cold leg fluid temperatures are shown in Figures 3 and 4, respectively. The temperatures converged by 60 s at 619.1°F in the hot leg and 559.3°F in the cold leg. The core inlet mass flow rate, shown in Figure 5 converged at a steady state value of 36,697 lbm/s within 50 s. The flow out of the pressurizer surge line converged at 0.0 lbm/s by 70 s as shown in Figure 6.

Steady state pressure histories for the core and the steam generator secondaries are shown in Figures 7 and 8, respectively. The core pressure converged by 45 s to a steady state value of 2287 psia. The steam generator secondary pressure at the steam separator converged by 60 s to a value of 992.6 psia.

The steady state fuel pin radial temperature profile at the hot spot is shown in Figure 9 compared to the desired values presented in Appendix B. The temperature profile was obtained by adjusting the gas gap conductance and the pin radial power profile. The hot pin temperature profile was used to adjust these parameters since only one unique fuel pin specification can be input to TRAC-PD2 for the core. The maximum difference between calculated and desired peak fuel pin temperature in all

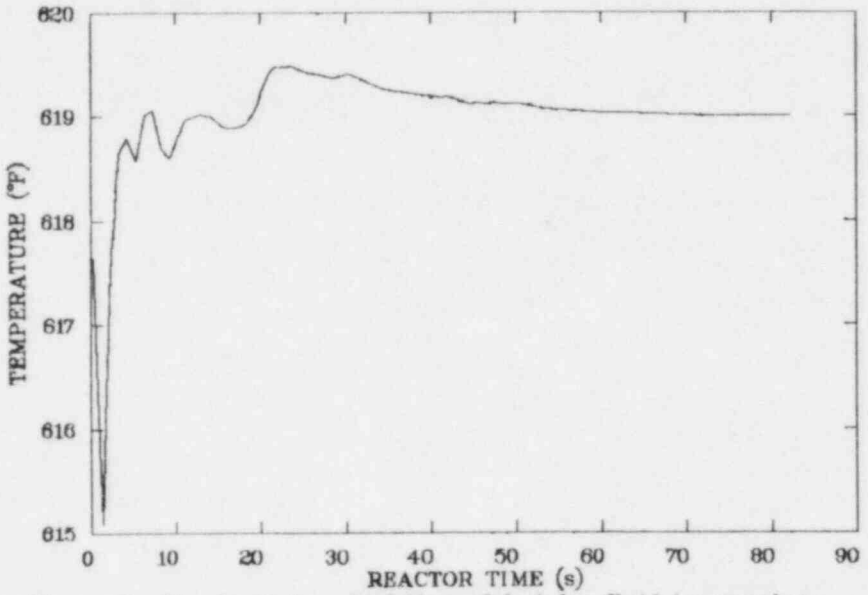

Figure 3. Steady state calculation of hot leg fluid temperature.

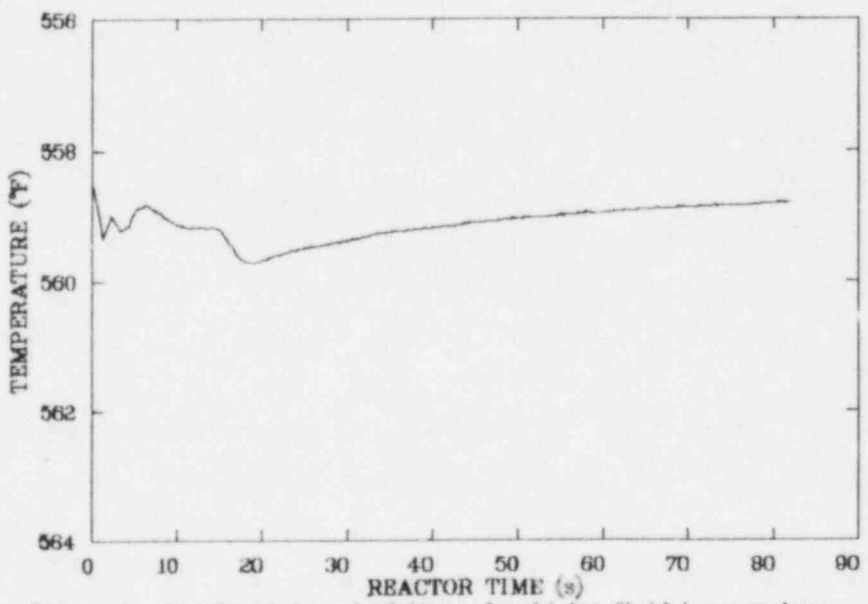

Figure 4. Steady state calculation of cold leg fluid temperature.

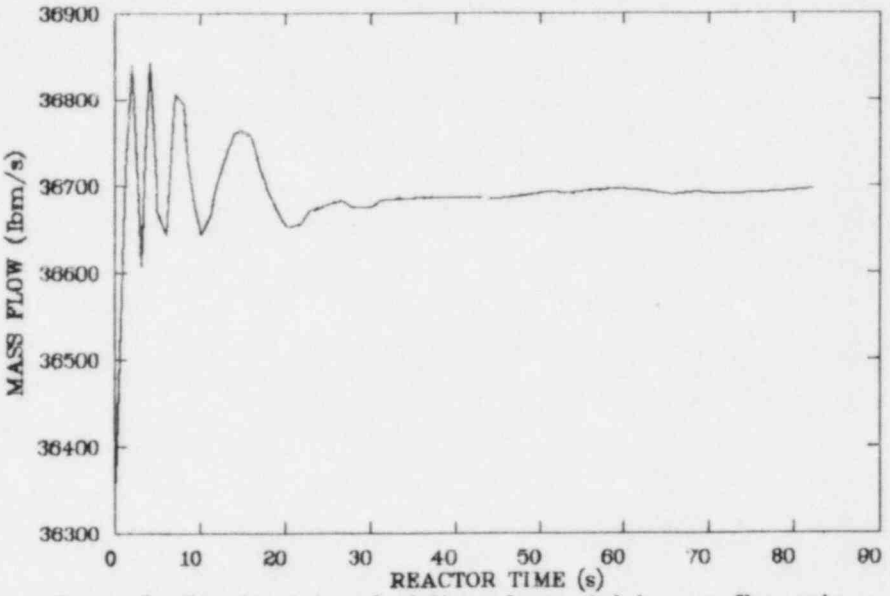

Figure 5. Steady state calculation of core inlet mass flow rate.

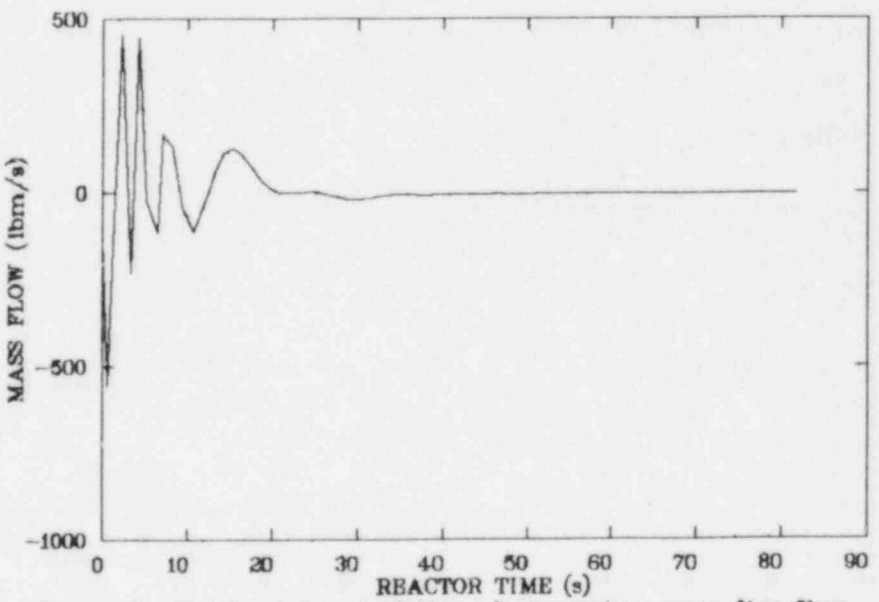

Figure 6. Steady state calculation of pressurizer surge line flow.

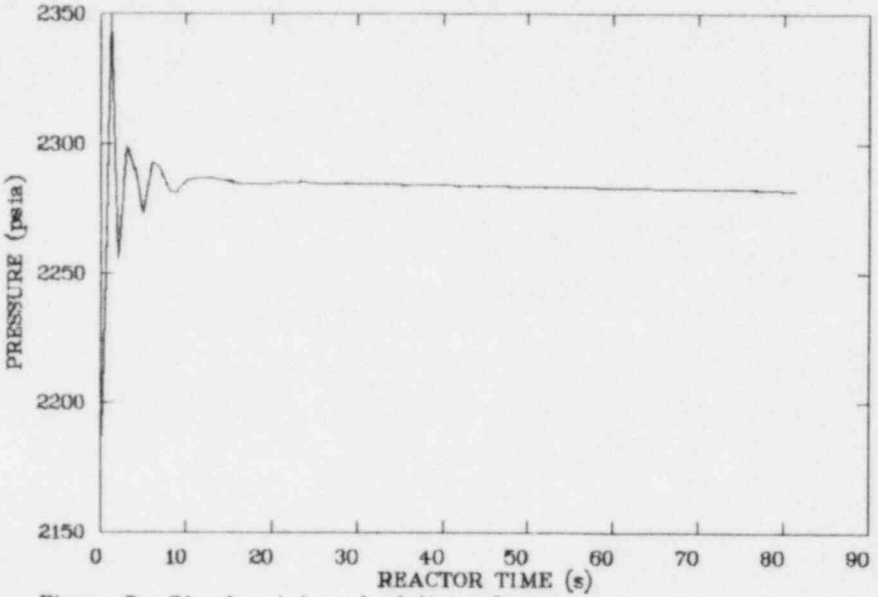

Figure 7. Steady state calculation of average core pressure.

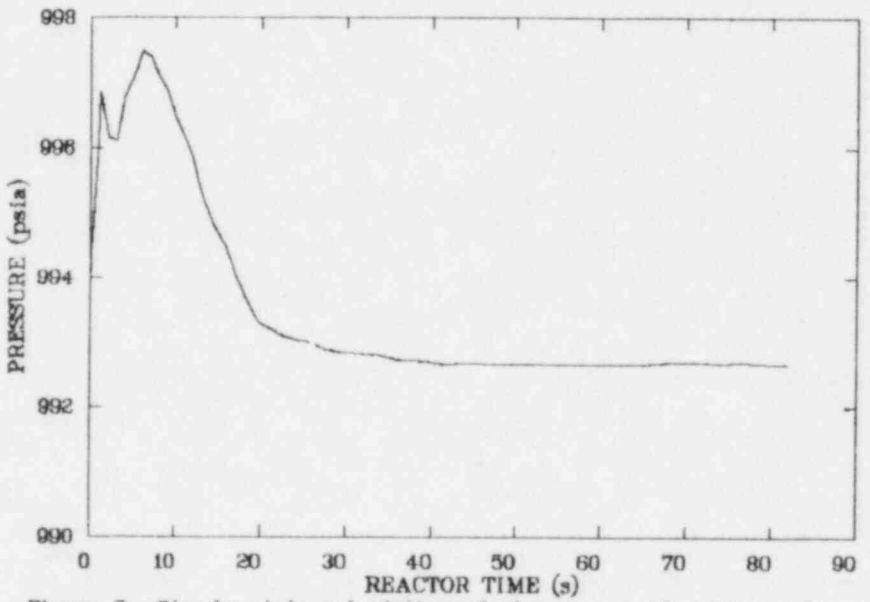

Figure 8. Steady state calculation of steam generator steam dome pressure.

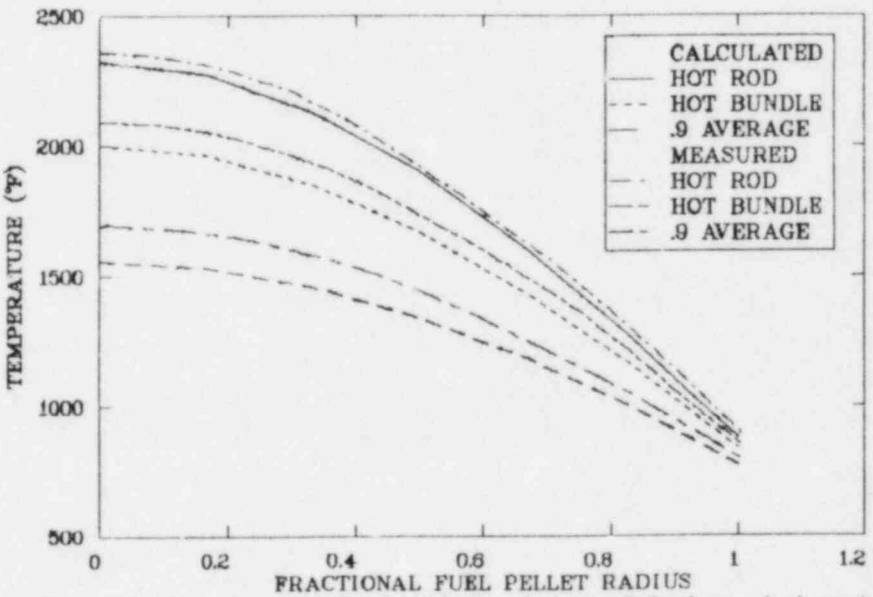

Figure 9. Comparison of calculated and desired fuel pin hot spot radial temperature profiles.

the rods occurred at the fuel centerline. The calculated centerline temperature was 1.5% lower than desired in the hot rod, 3.5% lower than desired in the hot bundle, and 6.7% lower than desired in the remaining 2/3 of the core. The uncertainty in the FRAPCON calculation was estimated to be on the order of ±10%. The fuel pin temperature profiles obtained for the TRAC-PD2 steady state analysis are therefore within the uncertainty of the desired fuel pin temperature profiles. Additionally, the error is a decreasing function of radius whereas the fuel volume increases as the square of the radius resulting in a net error in the pin stored energy less than that derived from centerline temperature differences.

A comparison of calculated and measured initial conditions for the RESAR-3S DECLG LOCA are presented in Table 3. Typically, all calculated values are within ±2% of the respective desired values specified in the Westinghouse plant library data. The primary difference between calculated and desired conditions occurred in the steam generator secondaries. A higher than specified feed flow and lower than specified recirculation ratio were used in the steam generator secondaries to increase the calculated primary to secondary heat transfer rate to the desired level.

5.2 TRAC-PD2 Transient Analysis

The transient calculation was initiated via restart from the steady state calculation with the renodalized broken loop cold leg described in Section 4.1. The calculation was completed to 50.8 s of transient requiring 18.17 cpu hours on a CDC 7600. The following section describes the transient calculation and presents the results, relating them to pertinent test data where possible.

The transient was run from 0.0 s to 19.1 s with the updates identified in Appendix B as MODPUMP and FXPUMP added to the code. Attempts to continue the calculation beyond 19.1 s were unsuccessful due to calculated water packing in the cold legs not being handled correctly by the water-packer logic in the code. Update FIX was added to the code to prevent this problem. Additionally, the following nodalization changes were also made at 19.1 s:

TABLE 3. COMPARISON OF CALCULATED AND DESIRED INITIAL CONDITIONS FOR THE RESAR-3S DECLG LOCA

Parameter	Desired	Calculated
Pressurizer steam dome pressure (psia)	2250.	2254.
Steam generator steam pressure (psia)	990.	992.
Hot leg temperature (°F)	617.8	619.0
Pump suction temperature (°F)	557.3	558.6
Cold leg temperature (°F)	557.6	558.9
Loop flow (lbm/s per loop)	9757.	9753.
Spray nozzle flow (lbm/s)	674.	661.
Core bypass flow (lbm/s)	1535.	1562.
Pump speed (rpm)	1186.	1190.
Main steam/feed flow (lbm/s)	1051.	1179.
Recirculation ratio	3.70	1.23

1. ECC liquid temperature was increased from 60°F to 90°F and ECC fill pressure was decreased from 2250 psia to 43.5 psia. This was required since pressure oscillations due to condensation in conjunction with the expansion of the liquid from 2250 psia to ~50 psia resulted in the code attempting to calculate pressures less than the lower limit of the water properties table.

2. The broken loop cold leg components (TEE 46 and PIPE 56) were renoded because the calculated primary system pressure had reached containment pressure. Component 46 was reduced from 16 cells to five cells and component 56 was reduced from 15 cells to four cells. The coarser noding accommodates flow reversals better than does the finer blowdown nodalization with less restriction on the time-step size.

The calculation was continued until 25.4 s at which time update FIXCON was added to the code in an attempt to increase the time step by modifying the condensation calculational scheme. The calculation was run to completion at 50.8 s with this code version.

The calculated sequence of major events are given in Table 4 for the RESAR-3S DECLG LOCA. The timing of these events was discussed in Section 3.2. The end of blowdown occurred at 18. s when the primary system pressure reached containment pressure. Lower plenum refill was completed by 28. s initiating core reflooding. The fuel rods were quenched at all locations by 46. s.

The calculated upper plenum and pressurizer pressures are shown in Figure 10. The upper plenum pressure dropped almost instantaneously from its initial value of 2270 psia to 1670 psia, the saturation pressure corresponding to the intitial hot leg temperature. The upper plenum pressure then decreased at a more gradual rate until reaching containment pressure at approximately 19 s. The slight leveling off in the depressurization rate between 2 and 5.9 s was the result of a core wide

TABLE 4. SEQUENCE OF EVENTS FOR RESAR-3S DECLG LOCA

Event	Time (s)
Break	0.0
Reactor trip	0.2[a]
Safety injection signal generated	1.1
Main steam/feedwater isolation begins	2.6
Charging and residual heat removal pumps activated	2.6
Broken loop accumulator injection begins	5.0
Main feedwater/steamline isolation complete	7.6
Safety injection pumps actuated	7.6
Intact loop accumulator injection begins	10.5
Pressurizer empties	12.0
End of blowdown	18.0
Beginning of reflood	28.0
Beginning of auxiliary feedwater flow	30.6
Core wide quench complete	46.

a. Shutdown due to void formation in core assumed to begin 0.2 s after break based on previous RELAP4 large break calculations of the Zion NSSS.

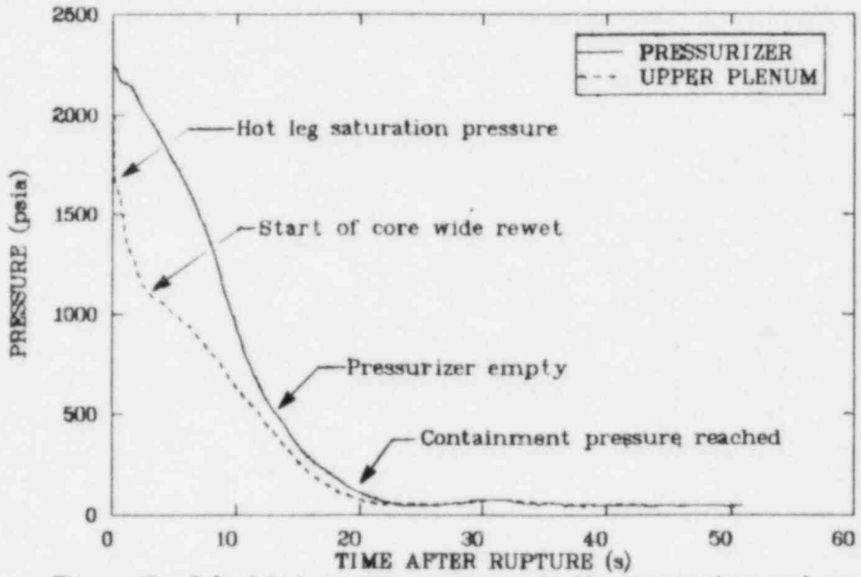

Figure 10. Calculated pressure response in the pressurizer and upper plenum.

rewet generating steam in the primary system. The pressurizer pressure remained above system pressure since the hotter liquid in the pressurizer flashed at a higher pressure. The pressurizer depressurized to near system pressure when the pressurizer emptied at 12 s.

The calculated break mass flow at the pump side and vessel side of the break are shown in Figures 11 and 12, respectively. The flows dropped rapidly during the initial 5 s of the transient as the cold leg fluid flashed near the break. The increase in pump side break flow at 5 s occurred when broken loop accumulator water reached the break and reduced the local void fraction at the break. The oscillatory behavior observed in the pump side of the break between 19 and 30 s resulted from slugs of ECC water being swept out the break. On the vessel side of the break, the break flow responded to the primary system depressurization after flashing approximately 2 s after the break. Intact loop accumulator water bypassing the core resulted in the flow oscillations observed between 15 and 20 s. The vessel side break flow stagnated following downcomer penetration at 20 s and remained essentially stagnant until the downcomer refilled at 30 s. Steam generation from fuel rod quenching in the core increased upper plenum pressure forcing water out the break between 30 and 35 s. Spillage out the break due to vessel refill was observed beyond 48 s.

The mass flow in the intact loops was typical of that shown in Figure 13 for intact loop 1 (refer to Figure 1 for loop designations). A sustained loop flow of 11,000 to 14,000 lbm/s per loop was calculated for the initial 3.5 s of the transient as a result of continued pump operation. The pumped loop flow exceeds the vessel side break flow during this period forcing fluid into the vessel. Pump head degredation resulting from void formation reduced the loop flows below vessel side break flow by 6 s. Following intact loop accumulator injection initiation at 10.5 s, the loop flows became very oscillatory due to the high steam condensation rates calculated in the cold legs.

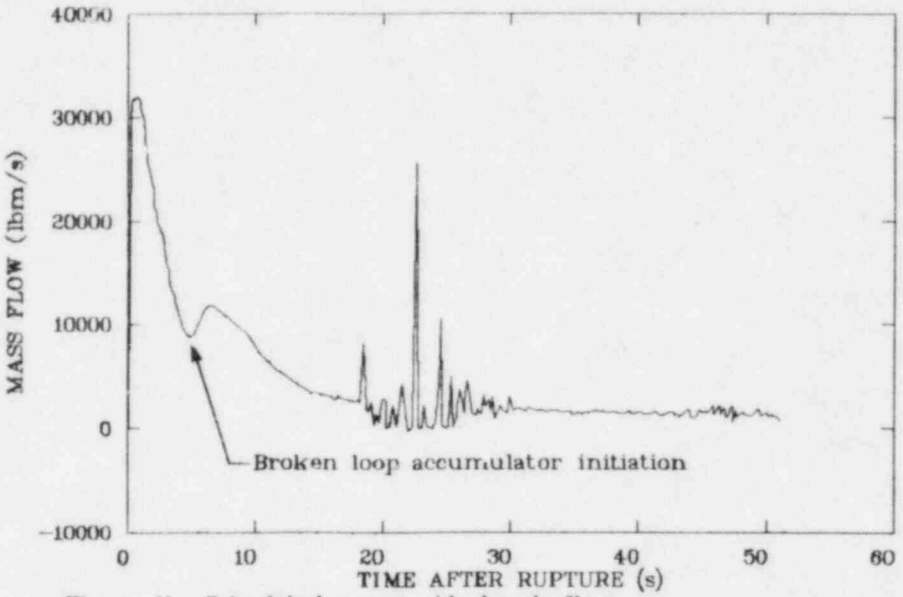

Figure 11. Calculated pump side break flow.

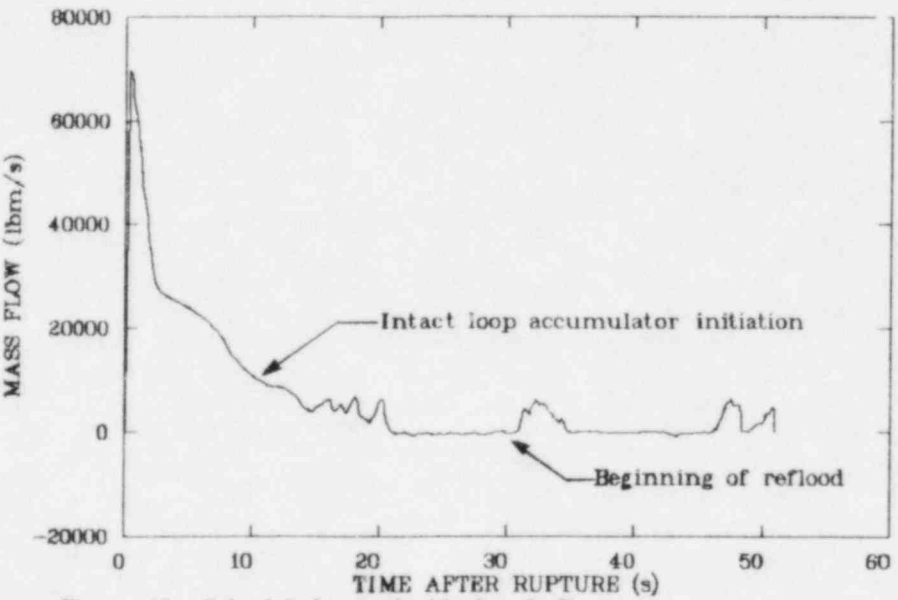

Figure 12. Calculated vessel side break flow.

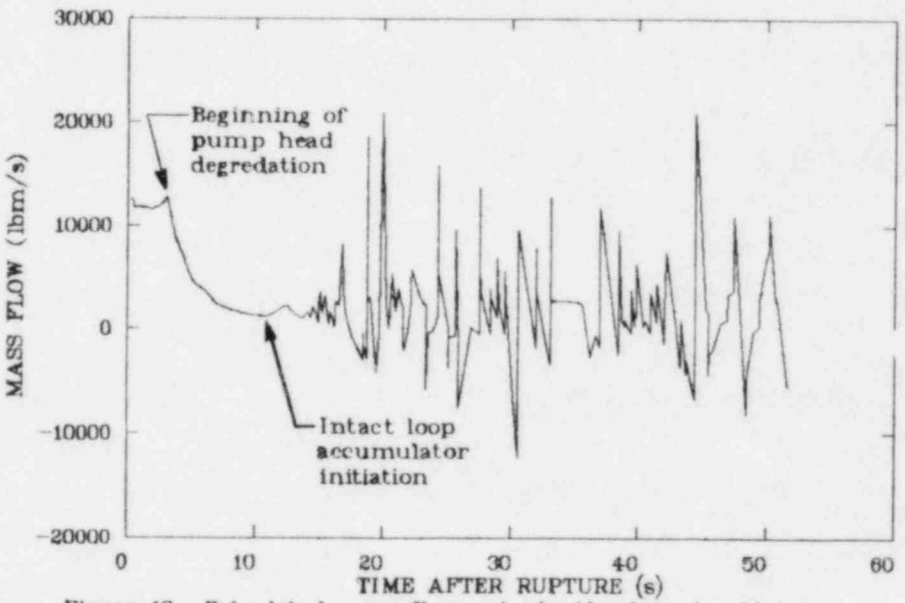

Figure 13. Calculated mass flow rate in the loop 1 cold leg.

The core inlet flow, shown in Figure 14, was initially negative as fluid was expelled from the core during the initial portion of the subcooled blowdown. The flow reversed due to the high loop mass flow rates producing a flow insurge into the core between 2 and 6 s. The flow then stagnated until the beginning of reflood at 28 s after which a net positive flow into the core was calculated.

The liquid fraction in the lower plenum and core is shown in Figure 15. The coolant inventory decreased rapidly as mass was expelled out the break and then recovered slightly during the period of high loop flow. The lower plenum began refilling after ECC bypass ended at 18 s with core reflood initiated at 28 s when the lower plenum was refilled. The core was completely reflooded by 43 s with subsequent boiling due to fuel rod quenching forcing some of the water back out of the core.

The calculated fuel rod cladding temperature response for the hot pin, high power region, and low power region of the core is shown in Figures 16, 17, and 18, respectively. The calculated temperature responses shown are representative of the core wide response for their respective radial location and pin power. CHF was calculated to occur between 0.8 and 1 s after the break over the entire length of the core in the high power region (inner ring which includes the hot pin) and between 1 and 1.5 s in the low power region (outer ring) of the core. The calculated surge of water into the core between 2 and 6 s after the break produced a core wide rewet away from the high power zones. Figure 18 shows that the lower power rods underwent a bottom-up rewet with the entire rod quenched by 4.5 s. The high power region rewet in a top down sequence with no rewet calculated below the 5 ft elevation. All rods were calculated to heat up during the remainer of the blowdown and refill with a core wide quench occuring with core reflood between 30 and 50 s. The final quench occurred 45 s after the break at the 5.4 ft elevation.

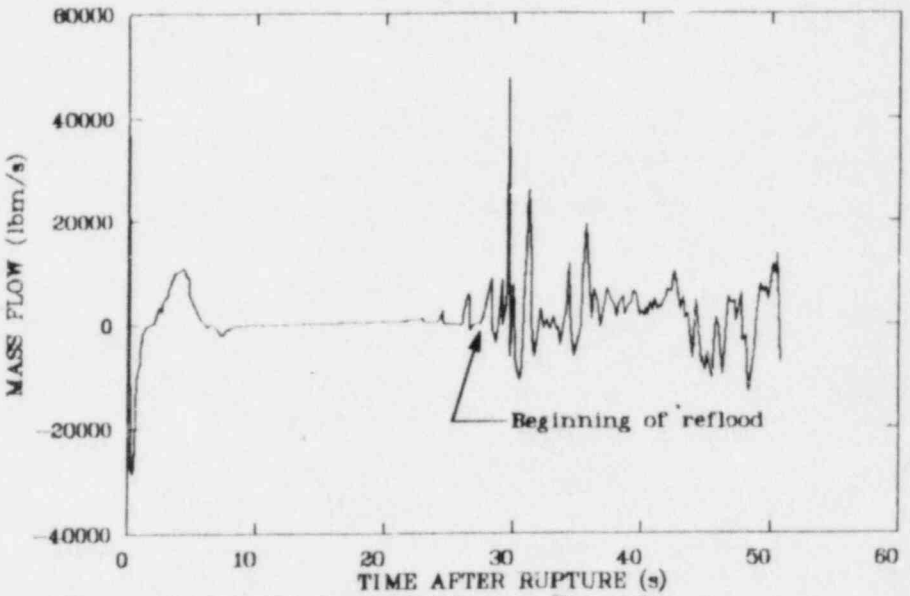

Figure 14. Calculated core inlet mass flow rate.

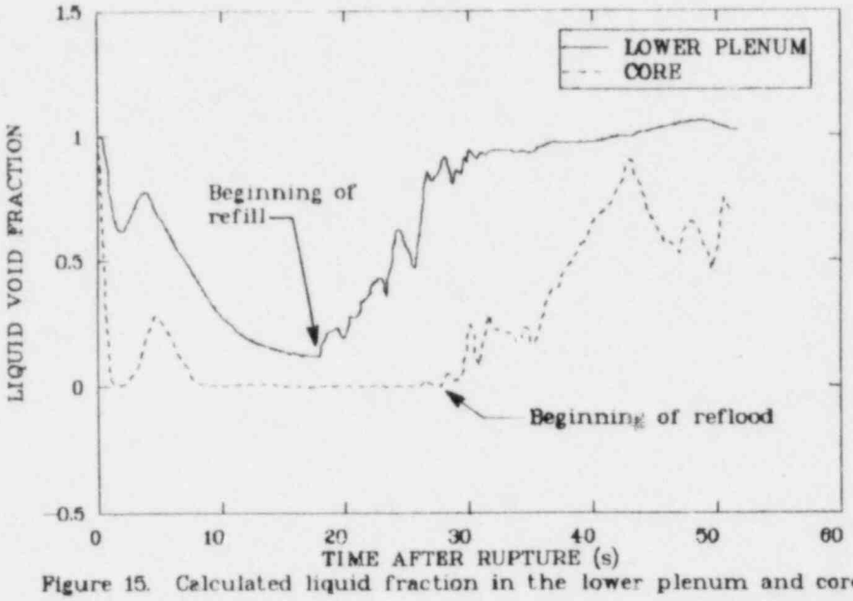

Figure 15. Calculated liquid fraction in the lower plenum and core.

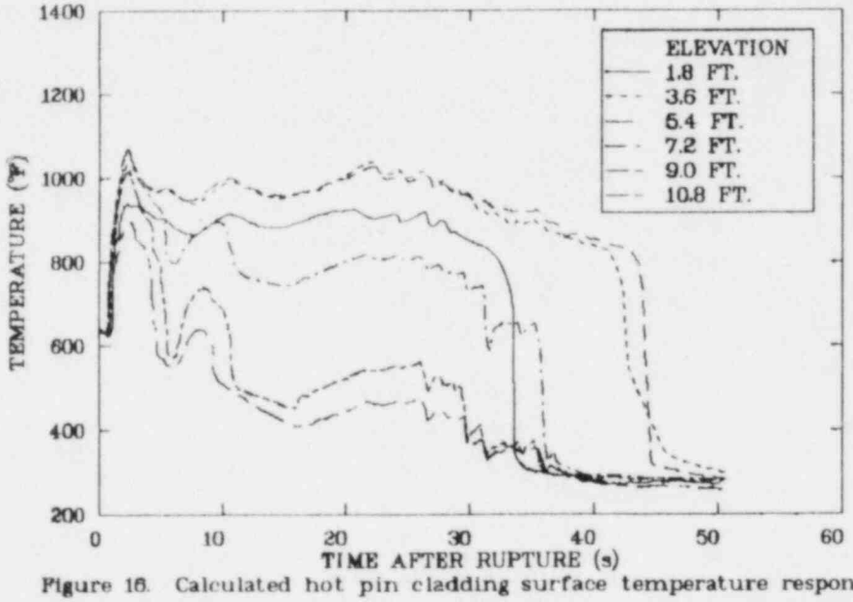

Figure 16. Calculated hot pin cladding surface temperature response.

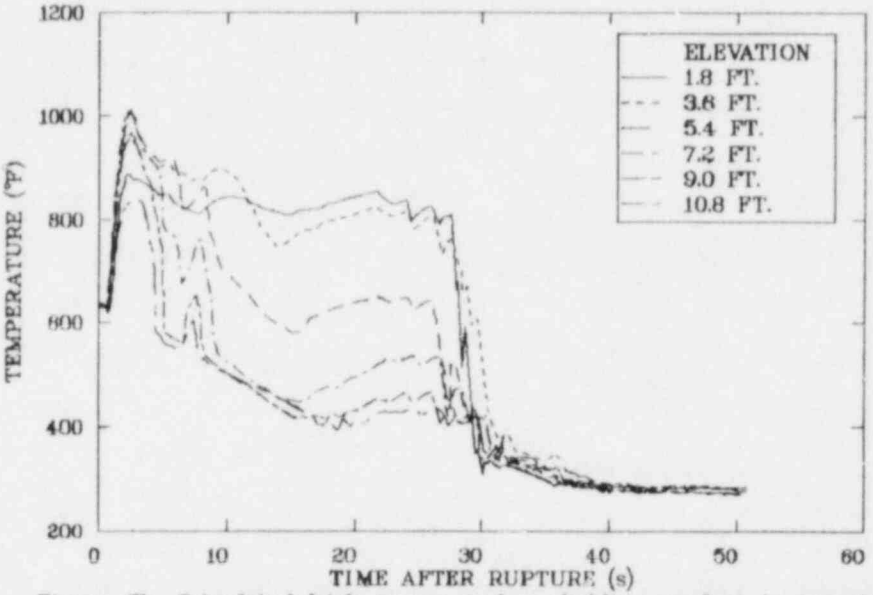

Figure 17. Calculated high power region cladding surface temperature response.

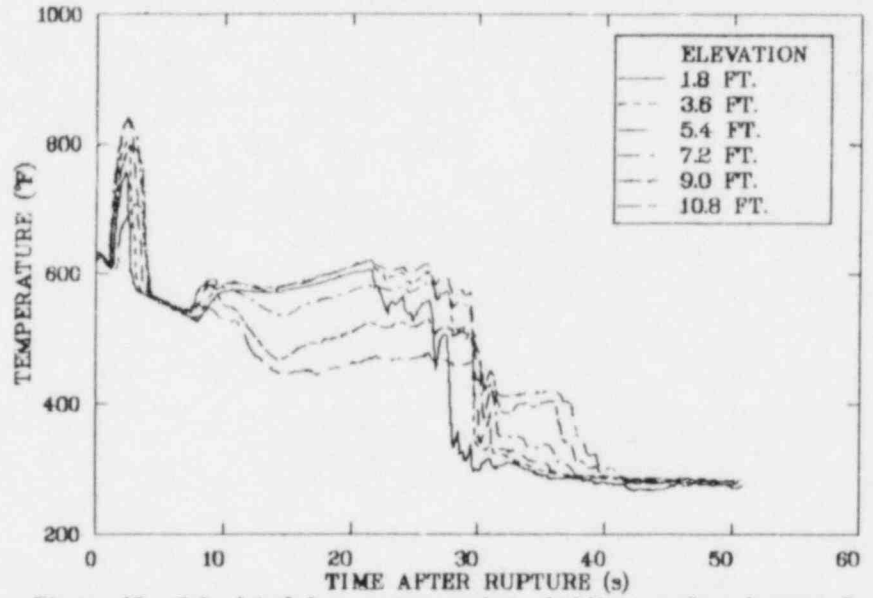

Figure 18. Calculated low power region cladding surface temperature response.

The maximum cladding surface temperature obtained during the transient was 1085°F calculated to occur 2.5 s after the break. The maximum cladding surface temperature was calculated to occur at all locations between 5.4 and 7.2 ft.

The calculated transient response was similar to the data from LOFT Experiments L2-2[5] and L2-3.[6] Both tests simulated double-ended offset shear breaks in the cold leg of a large pressurized reactor. Experiment L2-2 was conducted at peak fuel pin power of 8.04 kW/ft and Experiment L2-3 at 12.0 kW/ft. The early fuel rod rewets in the lower power regions of the core are typical of the results observed in both LOFT tests. Measurements showed the peak cladding surface temperature being attained between 5 and 6 s after rupture followed by combinations of bottom-up and top-down return to nucleate boiling. Measured peak cladding temepratures of 1186°F at 12.0 kW/ft (Experiment L2-3) and 960°F at 8.04 kW/ft (Experiment L2-2) bracket the TRAC-PD2 calculation for RESAR-3S of 1085°F at 9.13 kW/ft. Final quench was measured to occur 44 s after break in Experiment L2-2 and 54 s after break in Experiment L2-3 which compares well with the TRAC-PD2 calculated final quench time of 46 s after break. The TRAC-PD2 calculated depressurization rate was faster than that measured for LOFT. Containment pressure was reached in the calculation by 19 s and measured to occur in LOFT Experiments L2-2 and L2-3 at approximately 38 s.

As discussed in Reference 3, the accuracy of predictions of final quench times with TRAC-PD2 is about ±125 s (two standard deviations) with the predominant trend in integral LOFT and Semiscale experiments being early prediction of hot spot quench. TRAC-PD2 tends to predict overcooling of the higher elevations in the core during reflood. As was stated in Section 2, TRAC-PD2 does accurately predict peak rod surface temperatures when they occur during blowdown. Experimental data have shown that peak cladding surface temperatures occur during blowdown as opposed to during the reflood portion of the transient for linear heat generation rates as high as 12.0 kW/ft. The combination of these facts indicates that the peak cladding temperature predicted by TRAC-PD2 is 1085 ± 144°F.

The system state at the end of the calculation indicated no potential for further core voiding and associated rod dryout. All rods have been quenched removing the stored energy from the fuel. The core liquid fraction is between 0.7 and 0.8 and the accumulators are still injecting. The system should stabilize on pumped ECCS after the accumulators empty.

5.3 Comparison to Licensing Analysis

The following section presents comparisons between the TRAC-PD2 "best-estimate" analysis and the Westinghouse "evaluation model" analysis of the consequences of a DECLG LOCA. The Westinghouse analytical results are in some instances only given for the blowdown or reflood portions of the transient.

The comparison of pressure in the upper plenum is shown in Figure 19. Following the early decompression to hot leg saturation, the TRAC-PD2 calculation predicted a much more rapid pressure drop before cold leg flashing than did the Westinghouse analysis. The TRAC-PD2 analysis predicted a somewhat faster depressurization during saturated blowdown, reaching containment pressure at 19 s as opposed to approximately 23 s in the Westinghouse analysis. The increase in depressurization rate after 16 s in the Westinghouse calculation corresponded to accumulator injection initiation. The combination of earlier pumped ECC availability and primary coolant pumps running in the TRAC analysis were primary reasons for the more rapid calculated depressurization rate in the TRAC-PD2 analysis. Additionally, the higher hot leg fluid temperature in the Westinghouse analysis resulted in a higher hot leg saturation pressure. Finally, the TRAC-PD2 calculated subcooled break mass flow rate was higher than that calculated for the Westinghouse analysis.

Comparisons of pump side and vessel side break mass flows are shown in Figures 20 and 21, respectively. The pump side break mass flow calculated by TRAC-PD2 was approximately 50% higher at the peak than that calculated by Westinghouse during subcooled blowdown. The TRAC-PD2 calculated

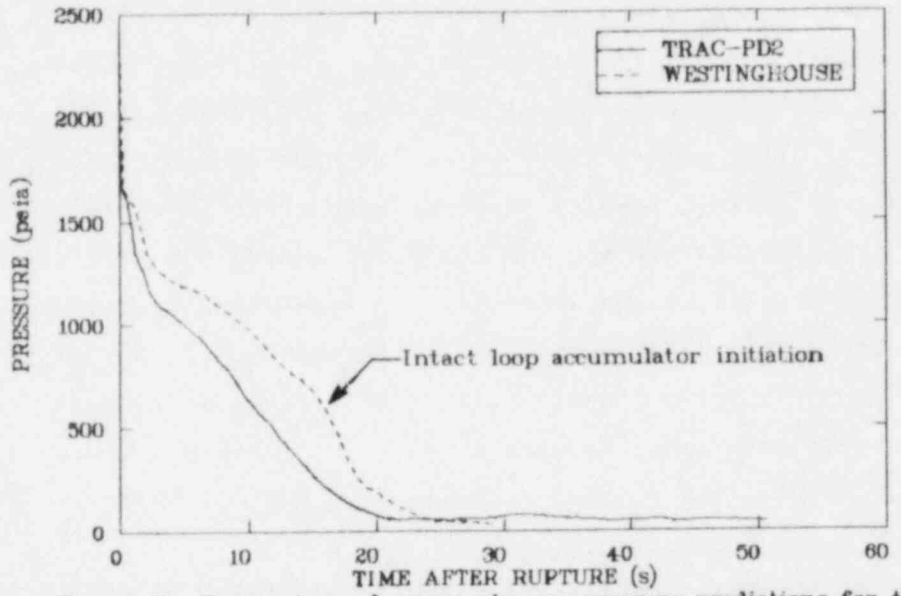

Figure 19. Comparison of upper plenum pressure predictions for the TRAC-PD2 and the Westinghouse analyses.

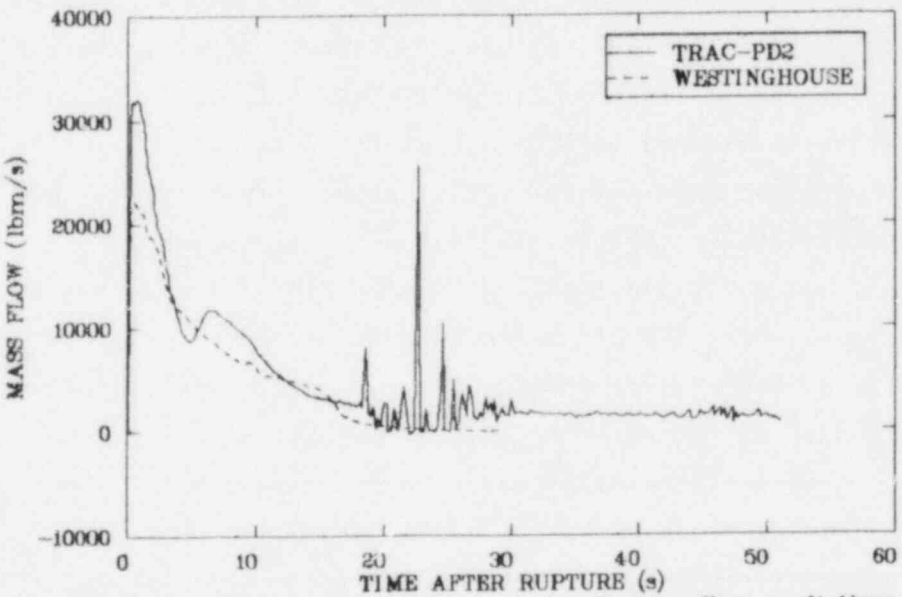

Figure 20. Comparison of pump side break mass flow predictions for the TRAC-PD2 and the Westinghouse analyses.

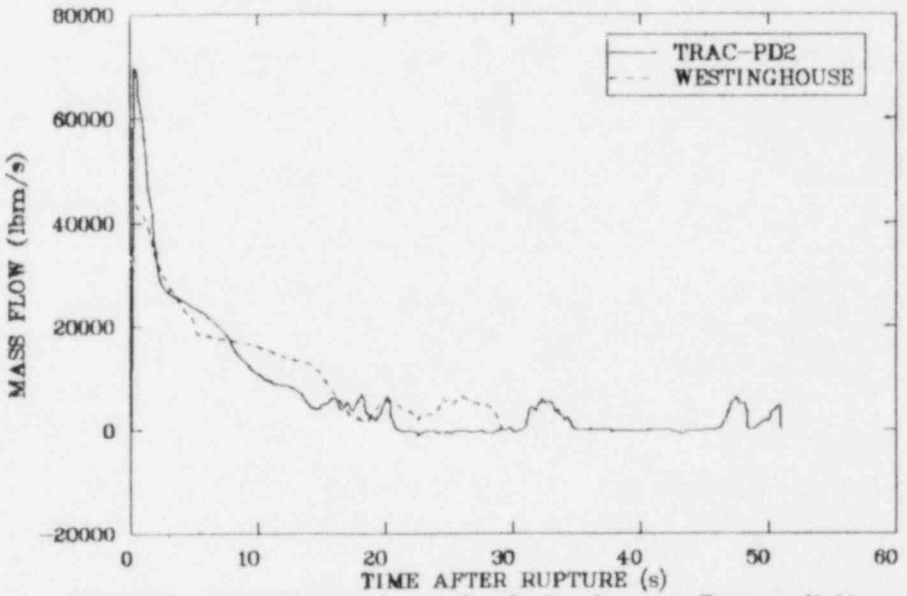

Figure 21. Comparison of vessel side break mass flow predictions for the TRAC-PD2 and the Westinghouse analyses.

increase in flow at 5 s due to broken loop accumulator flow initiation was not predicted by the Westinghouse analysis since Westinghouse did not model broken loop ECC injection. The difference between calculated pump break mass flow beyond 19 s was also due to ECC flow in the broken loop for the TRAC-PD2 analysis and none in the Westinghouse analysis. The vessel side break mass flow comparison showed similar trends to the pump side break mass flow with the TRAC-PD2 peak subcooled blowdown mass flow rate 50% greater than that calculated in the Westinghouse analysis. The Westinghouse analysis calculated a higher saturated mass flow than did the TRAC-PD2 analysis during the saturated portion of the blowdown due to the higher primary system pressure in the Westinghouse analysis. The difference in the calculated peak subcooled break mass flow rates may be due to Westinghouse applying the discharge coefficient of 0.6 during this region which would effectively yield a smaller break area than that used in the TRAC-PD2 analysis.

Comparisons of accumulator delivery rates are shown in Figure 22 for total intact loop accumulator flow. Due to the lower calculated primary pressure in the TRAC-PD2 analysis, the accumulator initiation time was 5.5 s earlier in the TRAC-PD2 analysis. Following accumulator initiation, the Westinghouse analysis calculated a higher accumulator mass flow rate than did the TRAC-PD2 analysis. The primary reason for the higher flow was the faster calculated primary system depressurization rate following accumulator initiation in the Westinghouse analysis (refer to Figure 19). A secondary effect may have resulted from the lower gas volume in the TRAC-PD2 analysis (due to the assumption of higher initial liquid inventory) resulting in a faster accumulator tank depressurization as the change in pressure is inversely proportional to the change in gas volume. The Westinghouse curve terminates at the calculated end of blowdown. Figure 23 shows the total intact loop ECC flow (accumulators plus pumped injection) during reflood for the Westinghouse analysis compared to the TRAC-PD2 analysis. The ECC flows were approximately equal during the early portion of reflood, starting at 30 s in the TRAC-PD2 analysis and 40 s in the Westinghouse analysis due to the higher pumped ECC available in the TRAC-PD2 analysis. The Westinghouse analysis predicted the accumulators

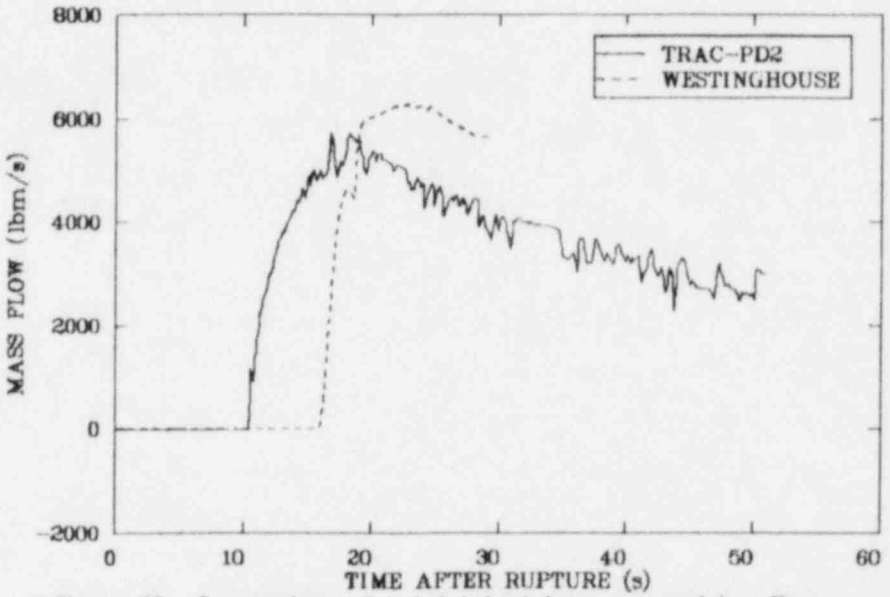

Figure 22. Comparison of total intact loop accumulator flow predictions for the TRAC–PD2 and the Westinghouse analyses.

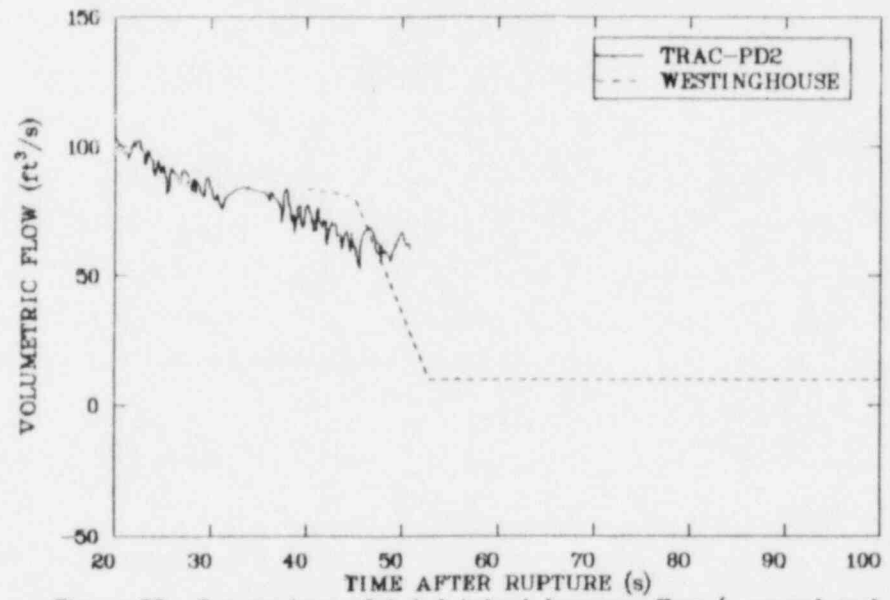

Figure 23. Comparison of total intact loop ecc flow (pumped and accumulator) predictions during reflood for the TRAC–PD2 and Westinghouse analyses.

would empty by 55 s with only pumped injection available whereas the TRAC-PD2 analysis had approximately 1/4 of the initial accumulator water volume available at the end of the analysis at 50.8 s.

Calculated core inlet mass flows are compared in Figure 24. The higher subcooled break mass flow calculated in the TRAC-PD2 analysis resulted in an initial larger negative flow out of the core than that calculated by the Westinghouse analysis. The insurge into the core beginning at 2 s in both calculations was significantly larger in the TRAC-PD2 analysis due to continued reactor coolant pump operation. Both analysis calculated essentially stagnant core inlet flow by 9 s continuing until the end of refill. The Westinghouse results are shown to the end of blowdown with stagnant core inlet flow assummed during refill. Figure 25 shows the comparison of core reflood rate for the Westinghouse calculation compared to that inferred from the TRAC-PD2 analysis. The TRAC-PD2 reflood rate was calculated from core inlet mass flow rate, core inlet fluid density, and effective core flow area. The TRAC calculation indicated a series of surges into the core with a sustained reflood rate of 10 to 20 in./s between 35 and 44 s. The Westinghouse analysis calculated a 2 s surge into the core beginning at 40 s and averaging 8 to 10 in./s decreasing to an average of 1 in./s for the remainder of the transient. The calculated core liquid level, shown in Figure 26, shows the rapid refilling of the core in the TRAC-PD2 analysis compared to the relatively slow reflooding rate calculated by the Westinghouse analysis. The net difference in the two analysis with respect to core reflooding rate hinges on the additional accumulator volume and higher pumped ECC flow in the TRAC-PD2 analysis as compared to that used in the Westinghouse analysis.

Comparisons of predicted cladding surface temperatures for the high power rod are shown in Figure 27 for the 6 ft elevation and Figure 28 for the 7.5 ft. elevation in the core. The 6 ft elevation was the last elevation quenched in the TRAC-PD2 analysis and the 7.5 ft elevation was the point of peak cladding surface temperature for the Westinghouse analysis. As stated in Section 5.2, the TRAC-PD2 analysis predicted the peak cladding surface temperature to occur at both the 6 and 7.5 ft

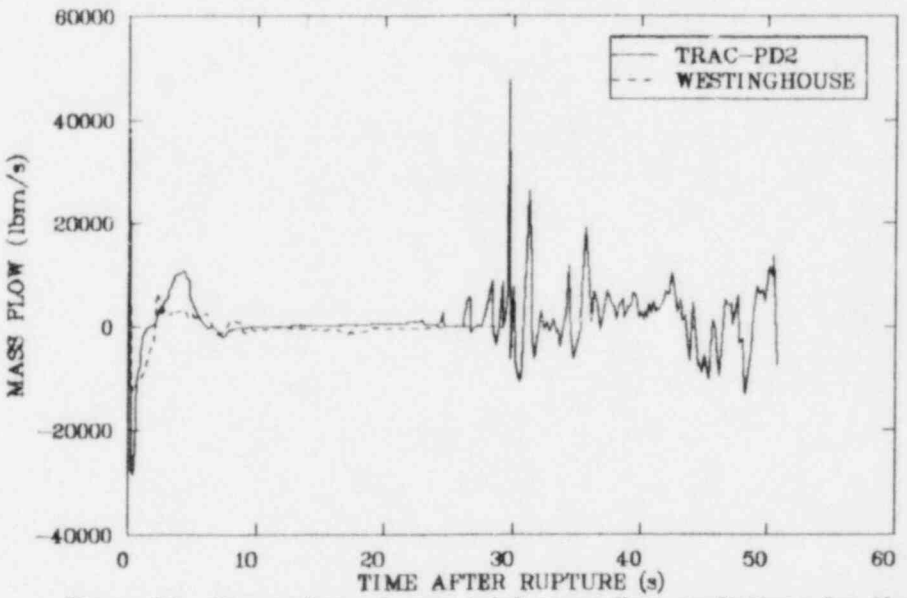

Figure 24. Comparison of core inlet mass flow predictions for the TRAC-PD2 and the Westinghouse analyses.

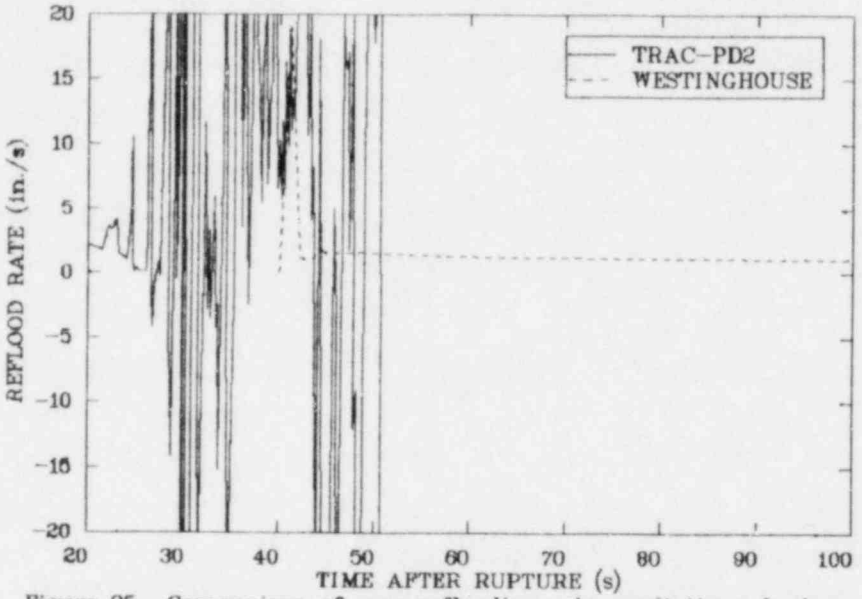

Figure 25. Comparison of core reflooding rate predictions during reflood for the TRAC-PD2 and the Westinghouse analyses.

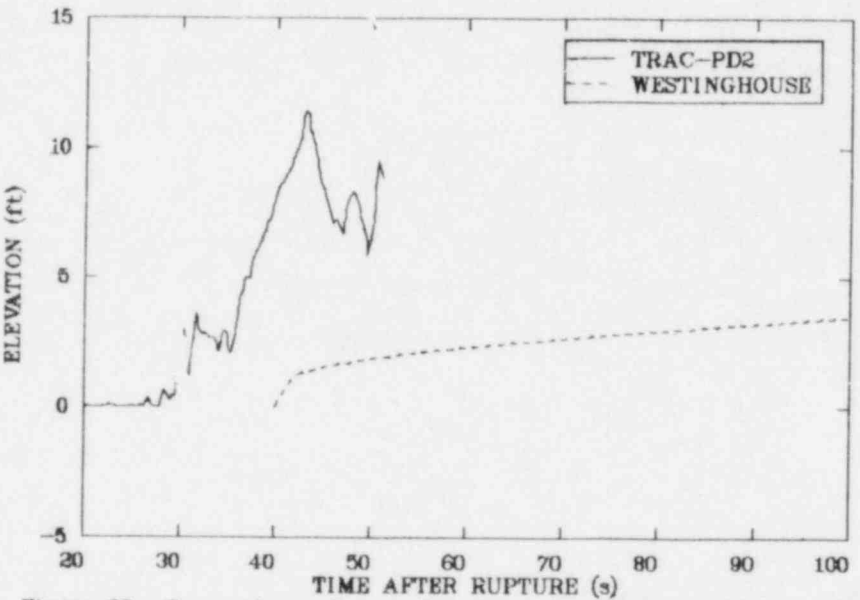

Figure 26. Comparison of core liquid level predictions during reflood for the TRAC-PD2 and the Westinghouse analyses.

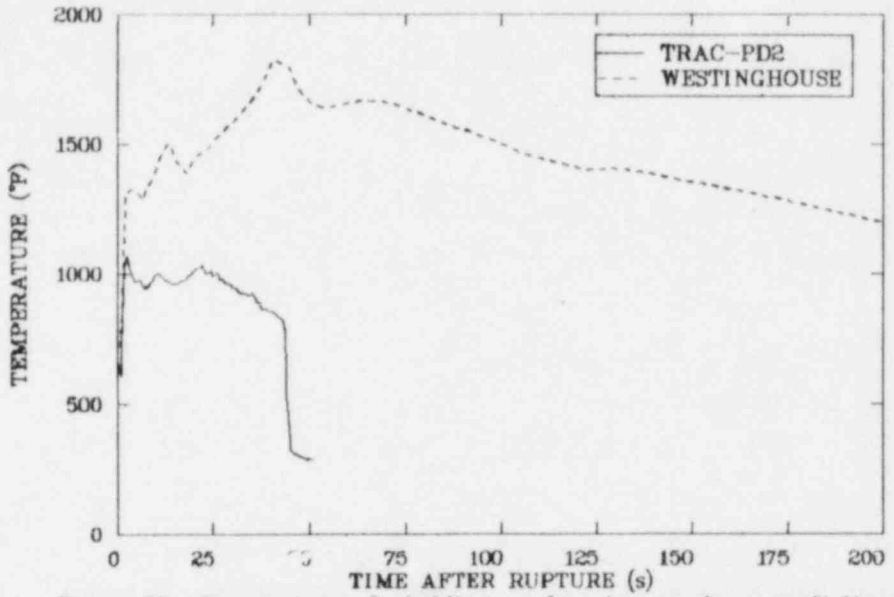

Figure 27. Comparison of cladding surface temperature predictions at the 6.0 foot elevation for the TRAC-PD2 and the Westinghouse analyses.

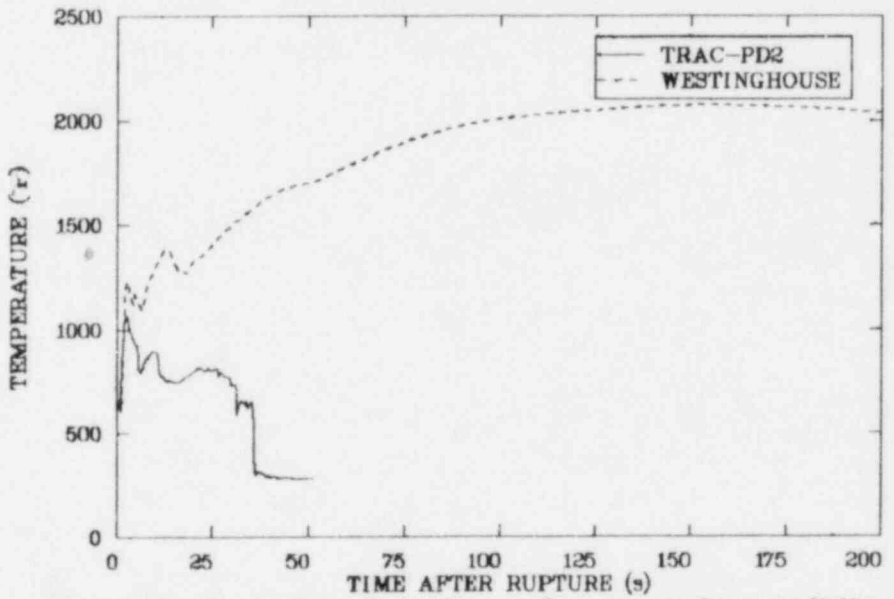

Figure 28. Comparison of cladding surface temperature predictions at the 7.5 foot elevation for the TRAC-PD2 and the Westinghouse analyses.

elevations. Lower core flow, higher peak power and the resultant higher stored energy in the Westinghouse analysis resulted in a higher cladding temperature at both elevations for the entire transient. The maximum cladding temperature calculated for the Westinghouse analysis was 2072°F and occurred during reflood at 155 s. The TRAC-PD2 analysis predicted a peak cladding temperature of 1085°F occurring during blowdown 2.5 s after the break.

Quantitative assessment of individual conservative assumptions used in the Westinghouse analysis was not possible due to the interdependence of many of the assumptions. The net result of the comparison, peak cladding temperature, shows a quantitative conservatism of 987°F. The difference was primarily due to higher initial fuel stored energy in the Westinghouse analysis, a conservative assumption, and lower core mass flow during the calculated majority of the transient. The lower core inlet flow calculated in the Westinghouse analysis resulted from the lack of pump driving head early in the transient, a conservative assumption concerning loss of offsite power. During reflood, the reduced core inlet flow in the Westinghouse analysis resulted from lower initial accumulator liquid volume and reduced ECCS delivery rates, both conservative assumptions.

6. CONCLUSIONS

The TRAC-PD2 analysis of the consequences of a large break loss of coolant accident in the RESAR-3S NSS assumming best estimate conditions provided information required to verify and quantify the conservatisms inherent in licensing analysis of limiting large breaks. The following conclusions are based in the analysis of the TRAC-PD2 results and comparisons to the analagous licensing analysis.

1. The TRAC-PD2 analytical results compared well with experimental results from large break loss of coolant experiments. The calculated transient resembles the data from LOFT Experiments L2-2 and L2-3. The predicted core thermal response was in excellent agreement with the measured response particularly in regard to location, timing, and magnitude of the peak cladding surface temperature.

2. Comparisons between the TRAC-PD2 "best-estimate" analysis and the Westinghouse "evaluation model" analysis verify the high degree of conservatism inherent in a licensing analysis. The results show that the combination of conservative assumptions resulted in a more severe transient in the Westinghouse analysis. The results of the TRAC-PD2 analysis when compared to the Westinghouse analysis showed a similarity in the calculated trends. Earlier accumulator emptying due to a lower initial accumulator liquid mass and reduced pumped ECCS delivery rates in the Westinghouse analysis resulted in a lower core reflooding rate than that predicted by the TRAC-PD2 analysis. The lower core flow and higher than expected peaking factors in the core for the Westinghouse analysis resulted in calculated peak cladding temperatures 987°F higher than those predicted by the "best estimate" TRAC-PD2 analysis. Due to the interrelationship of the conservative assumptions used in the Westinghouse analysis, it was not possible to define a quantitative effect of individual assumptions.

REFERENCES

1. 10 CFR Part 50, "Acceptance Criteria for Emergency Core Cooling Systems for Light-Water-Cooled Nuclear Power Plants," Federal Register, Vol. 39, No. 3, January 4, 1974.

2. TRAC-PD2, An Advanced Best-Estimate Computer Program for Pressurized Water Reactor Loss of Coolant Accident Analysis, NUREG/CR-2054, LA-8909-MS, April 1981.

3. F. Odar, "Independent Assessment of the TRAC-PD2 Code," U.S. Nuclear Regulatory Commission, ANS Topical Meeting, Kiamesha, New York, September 22-24, 1982 (to be published).

4. Aerojet Nuclear Company, RELAP4/MOD5--A Computer Program for Transient Thermal-Hydraulic Analysis of Nuclear Reactors and Related Systems, Volume I, ANCR-NUREG-1335, September 1976, page 200.

5. M. McCormick-Barger, Experiment Data Report for LOFT Power Ascension Test L2-2, NUREG/CR-0492, EG&G Idaho, February 1979.

6. P. G. Prassinos et al., Experiment Data Report for LOFT Power Acsension Experiment L2-3, NUREG/CR-0792, EG&G Idaho, July 1979.

APPENDIX A

TRAC-PD2 UPDATES USED FOR THE RESAR-3S CALCULATION

APPENDIX A

TRAC-PD2 UPDATES USED FOR THE RESAR-3S CALCULATION

The basic code used for the RESAR-3S calculation was TRAC-PD2/MOD1. The code was ran at Los Alamos National Laboratory where it is identified as TRAC-PD2/MOD1 Version 27.0. During the course of the RESAR-3S large break analysis, a series of updates were applied to the code. Section 5.2 of this report discussed the updates with respect to when in the transient they were applied. The microfiche at the end of this appendix contains a complete listing of the updates used. The updates are divided into the following groups:

1. TKVALVE--adds a new valve option to model the LOFT steam flow control valve. The update modifies the check valve option only when the new valve option is requested.

2. GEO--summarizes the actual input volumes and flow areas for the VESSEL component implied from the user input fractions. The update provides information in the output file only and does not affect the calculation.

3. MODPUMP--changes the fluid conditions and velocity used to evaluate the homogeneous pump curves from the boundary arrays to Cells 1 and 2 in the PUMP component and the pump interface between Cells 1 and 2.

4. FXPUMP--limits the growth in the pump momentum source and prohibits sign change in adjacent time steps.

5. FIX--modifies the water-packer logic to pick up calculated water packing that was being missed by the coding.

6. FIXCON--changed the condensation model by modifying the velocity used in the condensation model to reduce condensation only if the liquid velocity was determined to be less than the vapor velocity.

APPENDIX B
FRAPCON-2 ANALYSIS FOR INITIAL FUEL CONDITIONS

E. T. Laats

APPENDIX B
FRAPCON-2 ANALYSIS FOR INITIAL FUEL CONDITIONS

The FRAPCON-2 steady state fuel rod behavior code[a] was used to estimate the initial conditions of the RESAR-3S fuel rods prior to the LOCA events analyzed in this study. First, the hot rod was modeled to operate at constant full power (29.9 kW/m peak power on the hot rod) to determine when during the rod lifetime that maximum centerline temperature and stored energy occurred. That time was found to be 10 days after initial startup, when fuel centerline temperature was about 25 K higher than at BOL. Then, the radial temperature profile and stored energy were determined for a typical hot bundle rod, a core average rod, and a rod operating at 90% of core average power.

Presented in this Appendix are a brief description of the FRAPCON-2 code, the input to the FRAPCON-2 code used for this analysis, and the results obtained.

1. FRAPCON-2 DESCRIPTION

The FRAPCON-2 code[1] calculates steady state thermal and mechanical behavior of light water reactor fuel rods under long-term irradiation conditions. FRAPCON-2 is a modular code containing isolated subcodes that model fuel temperatures, considering fuel cracking and relocation; fuel and cladding deformation, including elastic and plastic cladding deformation and creep; and rod internal pressure, including fission gas release effects.

Fuel, cladding, and internal gas properties are modeled by a materials properties subcode, MATPRO-11.[2] FRAPCON-2 also includes the FRAIL-5 subcode that determines the probability of fuel rod failure.

---

a. Idaho National Engineering Laboratory Configuration Control Number H019882B.

Input to FRAPCON-2 includes axial nodalization and fuel rod design parameters, which are to be supplied by the user. The rod operating history, which specifies the system coolant conditions, axial power distributions, and time dependent rod average power, must also be given.

A detailed description of FRAPCON-2 is available in References B-1 and B-2.

2. FRAPCON-2 INPUT

The FRAPCON-2 input deck for the hot rod (with Westinghouse proprietary information deleted) is listed on Table B-1. The required input to model the rod and coolant channel geometry represent the RESAR-3S 17 x 17 rod and bundle configurations. The FRAPCON-2 model options selected were the PELET deformation model and the FASTGRASS fission gas release model. These selections are based on the recommendations in References B-3 and B-4.

The corewide power distributions used in this study represented values reported in the RESAR-3S Safety Analysis Report. The rod axial power distribution attained a peak-to-average ratio of 1.19 and a core wide radial peak-to-average ratio of 1.41. Thus, the peaking factor at the hot location of the core hot rod was 1.41 x 1.19, or 1.678. For the average rod in the core hot assembly, the radial peak-to-average ratio was assumed to be 1.20, rather than 1.41 as used for the hot rod. The radial power distribution within the fuel pellets was calculated within the FRAPCON-2 code. That power distribution is illustrated in Figure B-1.

To determine the time during operation when maximum stored energy occurred, the power history of the hot rod was divided into two parts. First, the rod was ramped to full power (9.13 kW/ft or 29.9 kW/m at the peak power elevation) at the rate of 3 kW/hr. Then, constant full power operation was maintained for 1000 hrs. It was noted from this calculation that maximum stored energy of the hot rod occurred at 10 days after startup. Then, the three other calculations were performed to represent an

TABLE B-1. FRAPCON-2 INPUT DECK.

```
ETL,SEA,P2,T77,EC12.
ACCNT,ID=ETL,ORG=2230,CHG=[redacted],BIN=TK9.
REL,CM=377000,EC=12.
ATTACH,FRPCN2,FRAPX,ID=BNWV1M3.
FRPCN2.
0
RESAR-3S CALCULATION -- HOT ROD
 $FRPCN
 IM =   20,NA =   12,NR =   11,NF =    5,NC =   4,MECHAN =1,NGASR=-2,
 $END
 $FRPCON
 COMP   =     0.,CPL    =0.16457,DCI    =.008357,DCO    = 0.0095,
 DE     =.01177,DEN    =  95.06,DISHSD=[redacted],DP     =.008192,
 DSPG   =[redacted],DSPGW  =[redacted],ENRCH  =    2.6,FGPAV  =[redacted],
 FLUX   =3.9E13,HDISH  =[redacted],HPLT   =0.01346,ICM    =       4,
 IDXGAS=       1,IPLANT=       1,IQ     =       0,JDLPR  =       1,
 JN     =      11,JST    =       1,NOPT   =       0,NSP    =       0,
 NUNITS=       0,ROUGHC=[redacted],ROUGHF=[redacted],TOTL   = 3.6585,
 VS     =  [redacted],
 CLDWKS=  [redacted],CREPHR=    10.,                  GRNSIZ=    10.,
 NPRINT=       1,PPMH2O=     0.,PPMN2 =    15.,RSNTR  =    93.2,
 TSINT  =  [redacted],
 GO(1)  = 3532.,
 TW(1)  = 565.,
 P2(1)  = 1.53E+7,
 QF(1)  = 0.27,0.97,1.13,1.19,1.19,1.19,1.18,1.14,1.10,0.91,0.22,
 X(1)   = 0.,0.366,0.732,1.098,1.463,1.829,2.195,2.56,2.93,
          3.29,3.6585,
 OMPY(1)= 0.1,3.0,6.0,9.0,12.0,15.0,16.06,17.84,18.0,21.0,
          21.41,24.0,8*25.16,
 TIME(1)=0.01,0.042,0.083,0.125,0.167,0.208,0.223,0.248,
         0.25,0.292,0.297,0.333,0.349,1.,5.,10.,15.,20.,25.,30.,
 $END
```

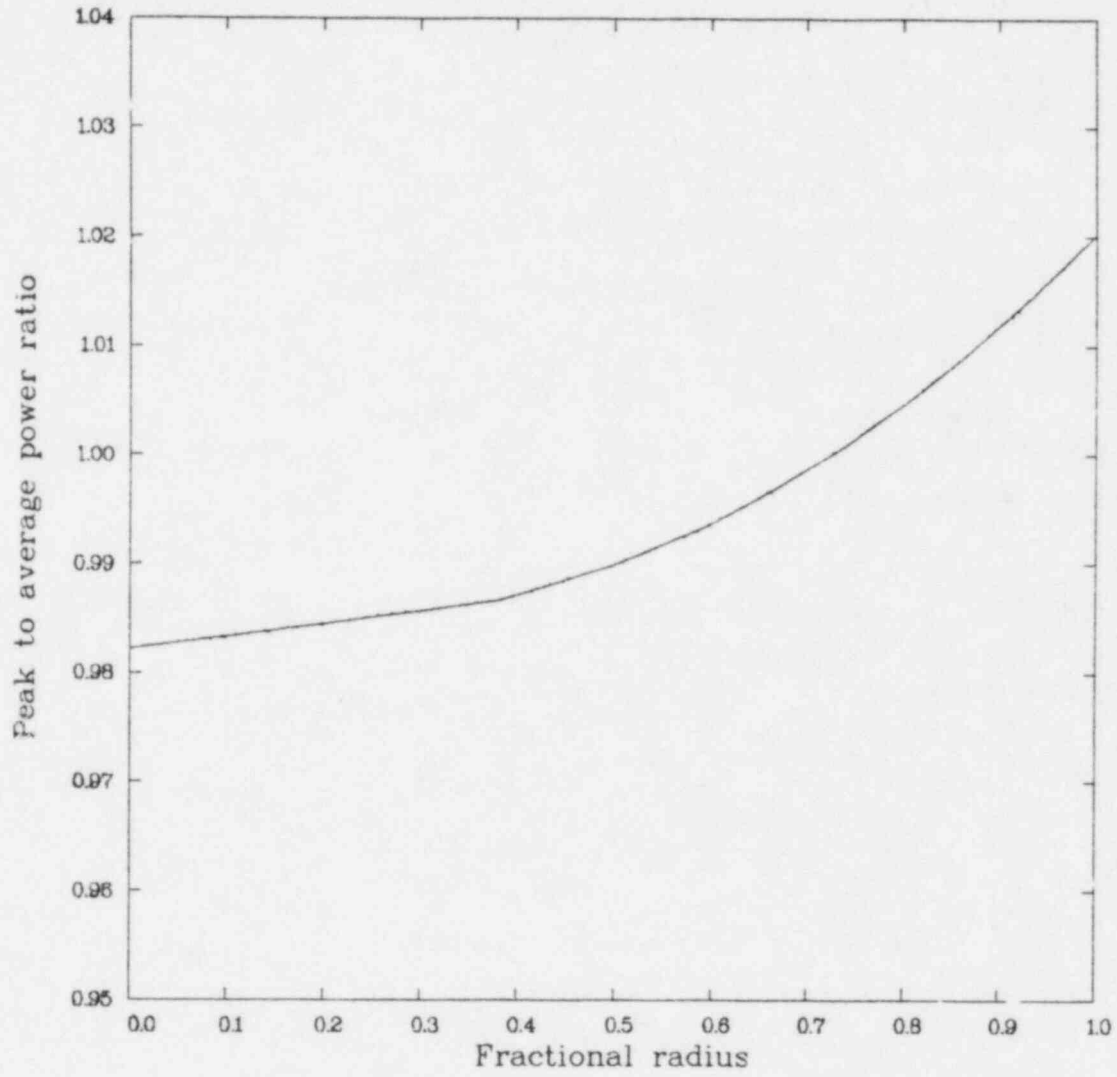

Figure B-1. Radial power distribution in the fuel pellets.

average rod in the hot assembly, a core average rod, and a rod operating at 90% of core average power. (These three calculations were needed as input to subsequent thermal-hydraulic calculations.) Each of the three calculations was also subjected to the 3 kW/hr startup ramp and subsequent constant power operation to 10 days. The radial temperature distribution noted at the end of the 10 day irradiation, was subsequently used to initialize the thermal-hydraulic calculations.

3. RESULTS

The results of the four FRAPCON-2 calculations (hot rod, hot assembly, core average, 90% of core average) are summarized in Figure B-2. Shown are four curves representing the radial temperature profile for each case, at the rod hot spot. These profiles were obtained at 10 days after startup. The fuel centerline temperature of each curve shown in Figure B-2, is plotted in Figure B-3 against local power.

Since maximum stored energy occurred at 10 days, no significant effects of long term irradiation were noted, such as fission gas release, cladding creepdown, and fuel densification. Thus, the boundary conditions and general state of the fuel rods, as subsequently modeled by the thermal-hydraulic codes, reflect fresh fuel rods. The only exception is decay heat, which was assumed to be 91% of the heat generated if the ANS 73 model was used.

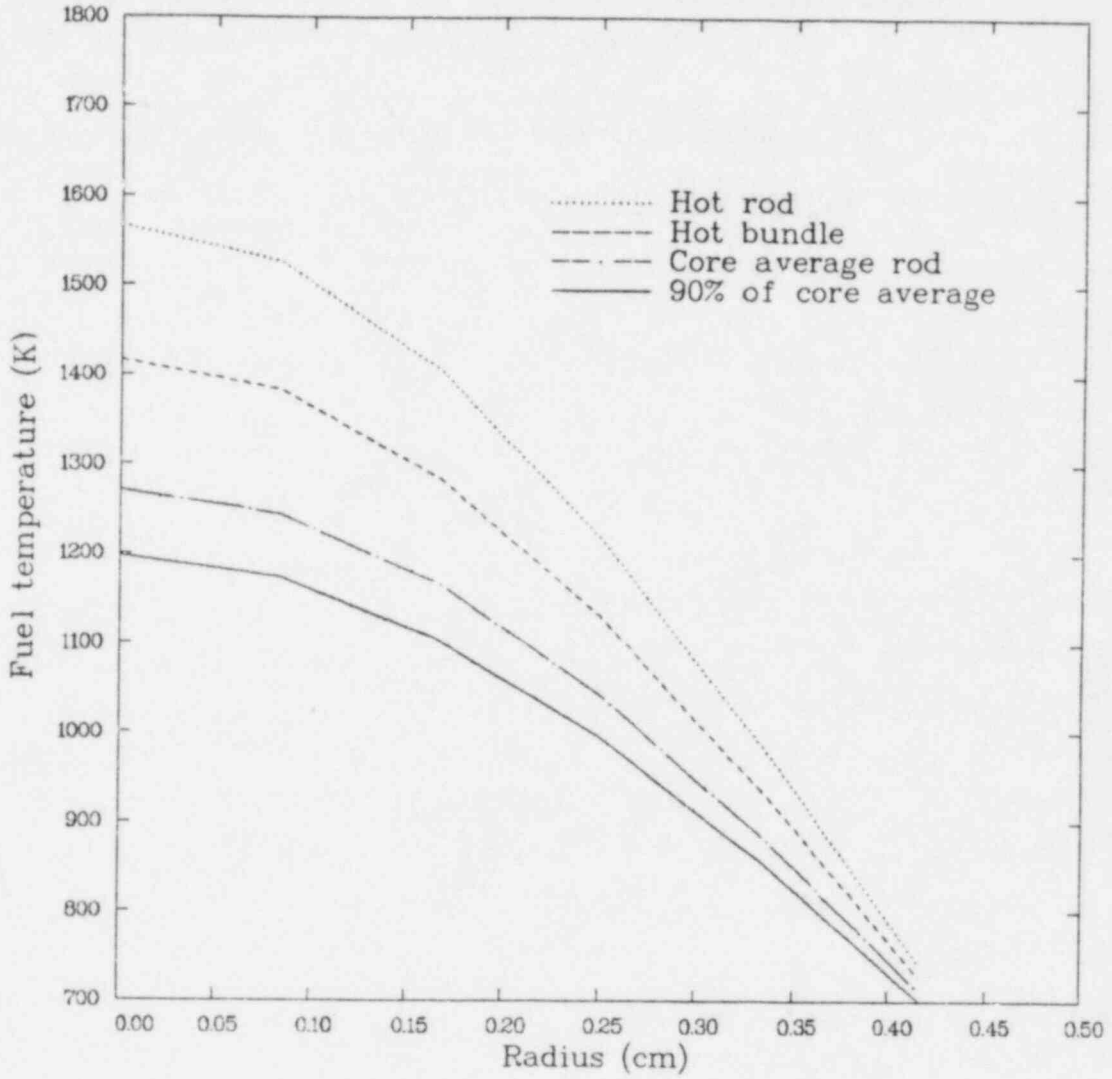

Figure B-2. Radial temperature profiles from FRAPCON-2 calculations.

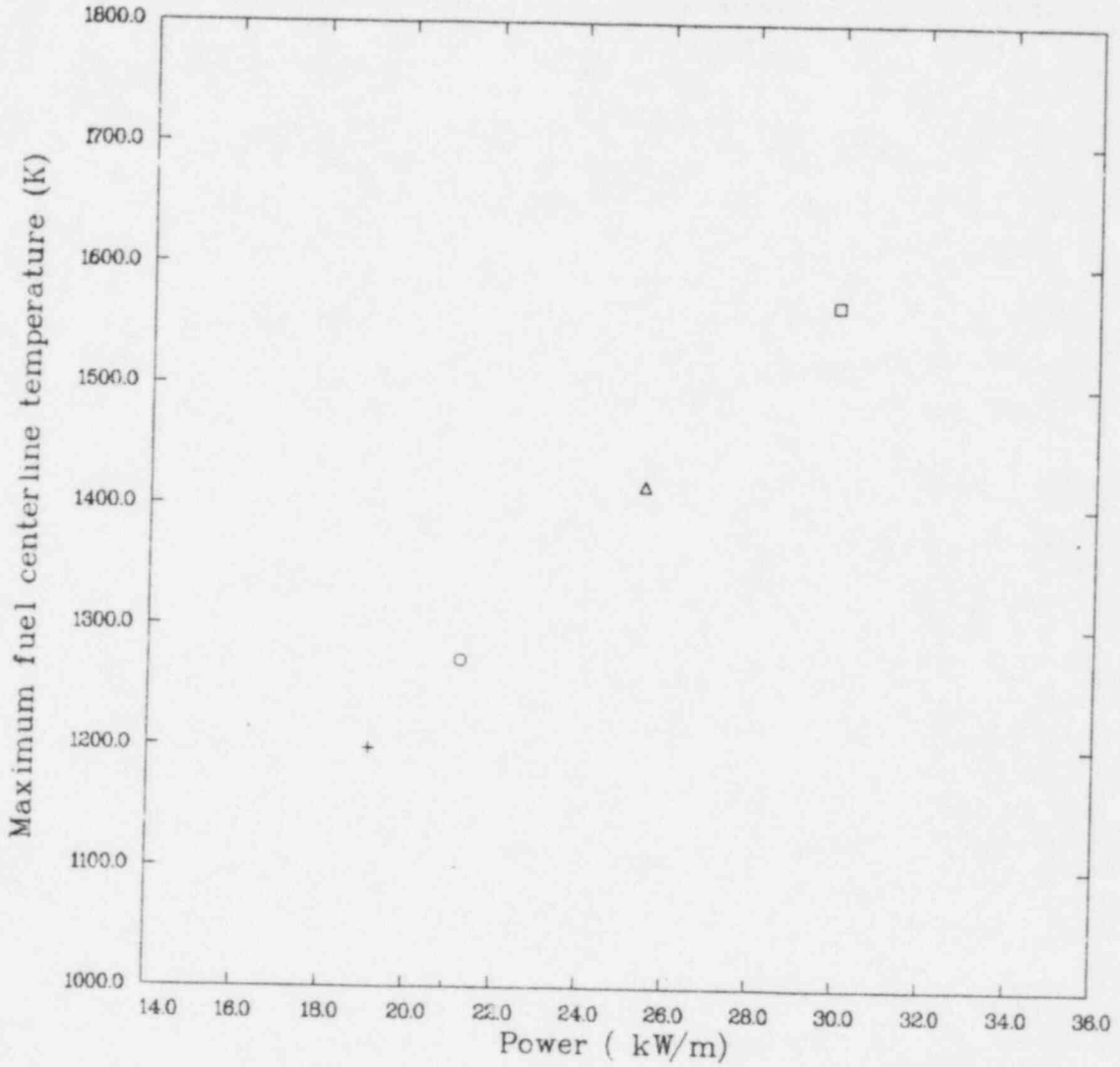

Figure B-3. Fuel centerline temperatures from FRAPCON-2 calculations vs. local power.

REFERENCES

B-1. G. A. Berna et al., FRAPCON-2: A Computer Code for the Calculation of Steady State Thermal-Mechanical Behavior of Oxide Fuel Rods, NUREG/CR-1845, December 1980.

B-2. D. L. Hagrman et al., MATPRO-Version 11 (Revision 1): A Handbook of Materials Properties for Use in the Analysis of Light Water Reactor Fuel Behavior, NUREG/CR-0497, TREE-1280, Rev. 1, February 1980.

B-3. E. T. Laats et al., Independent Assessment of the Steady State Fuel Rod Analysis Code FRAPCON-2, EGG-CAAP-5335, January 1981.

B-4. G. A. Berna et al., FRACPON-2 Development Assessment, NUREG/CR-1949, PNL-3849, July 1981.

APPENDIX C
QUALITY ASSURANCE PROCEDURE FOR DEVELOPMENT OF THE TRAC-PD2 RESAR-3S LARGE BREAK MODEL

APPENDIX C
QUALITY ASSURANCE PROCEDURE FOR DEVELOPMENT OF THE TRAC-PD2 RESAR-3S LARGE BREAK MODEL

The following is a quality assurance procedure that was developed, and followed, to assure the accuracy of the TRAC-PD2 RESAR-3S large break model.

1. System Nodalization Diagram--Based on FSAR information and knowledge of the transient to be run, a complete system nodalization diagram is constructed. All components and subsystems required for the calculation are included in the nodalization diagram. This process allows a straightforward determination of the type of data/information required to compile a plant data base (Step 2).

2. Plant Data Base--A plant data base is compiled to include all the data/information required to develop the plant model. The contents of the data base are of the form of actual plant drawings, technical specifications, operating manuals, FSARs, etc. (or copies of the same), and are limited to first hand sources (if possible). This step allows checking of all data/information back to an original source, rather than relying on second hand information. The data base also includes a table of contents that uniquely specifies all material contained therein. The table of contents lists all drawings by drawing number and revision number (if any), and all other sources of data/information by title, date, and revision number (if any). The table of contents is sufficiently detailed to allow duplication of the plant data base by an independent party if required.

3. Calculation Worksheets--A set of worksheets, which completely document all the calculations required to develop the input model, is compiled. Data used in a calculation are referenced to a drawing or other source of data listed in the plant data base (Step 2). Each calculation is written out in sufficient detail

to allow easy checking, and any assumption required in the calculation or any "special method" required to derive a given quantity are clearly indicated. If a calculation is a revision of a previous calculation, it is so stated on the worksheet, and the reason for the change is included. Both the initial calculation worksheet and the revised calculation worksheet are kept as part of the worksheet package.

4. Input Deck--The input deck is developed directly from the worksheets compiled in Step 3.

Once the above steps have been completed, the checkout of the system model proceeds as follows:

1. All data used in the calculation worksheets are checked and varified against the references in the plant data base.

2. All calculations are checked for accuracy and completeness.

3. Input deck values are checked against the values developed in the worksheets.

Notification that the calculation worksheets has been checked for accuracy is included on each worksheet by affixing the reviewers name and date (i.e., CHECKED BY _____, DATE _____). The "checked" status on the worksheet means both the calculations and initial data have been checked. Notification that the input deck has been checked for accuracy is included at the start of the input deck, along with the warning that no changes are to be made which would alter the plant model portion of the input, without first providing the appropriate calculation worksheet and input from revisions, and going through the checkout procedure (listed above) for each revision. By following this procedure, the continued accuracy of the input deck is assured.